# CORRECTING FOR PALEOMAGNETIC INCLINATION SHALLOWING IN MAGNETITE-BEARING CLAY-RICH SOFT SEDIMENTS WITH THE AID OF MAGNETIC ANISOTROPY AND UNIAXIAL COMPRESSION EXPERIMENTS

NEIL BRADBURY

# CORRECTING FOR PALEOMAGNETIC INCLINATION SHALLOWING IN MAGNETITE-BEARING CLAY-RICH SOFT SEDIMENTS WITH THE AID OF MAGNETIC ANISOTROPY AND UNIAXIAL COMPRESSION EXPERIMENTS

by

Neil Bradbury, B.Sc. Hon.

A Thesis submitted to the

School of Graduate Studies

in partial fulfillment of the

requirements for the degree of

Master of Science

Department of Earth Sciences

Memorial University of Newfoundland

April 2005

St. John's Newfoundland

## ABSTRACT

The remanence inclination, $I$, of magnetite-bearing sediment can be shallower than the inclination of the Earth's magnetic field, $I_{||}$, at the time of deposition due to burial compaction. Compaction also induces a magnetic anisotropy which can be used to correct for inclination shallowing. Theory predicts an approximately linear relation between $\tan I/\tan I_{||}$ and the sediment's remanence anisotropy parameter $ARM_{min}/ARM_{max}$ (the ratio of intensities of anhysteretic remanence given identically perpendicular and parallel to the bedding plane of the sediment). The slope of this line depends on the average remanence anisotropy parameter of the sediment's magnetite particles, $ARM_{\perp}/ARM_{||}$, (the ratio of intensities of anhysteretic remanence applied identically perpendicular and parallel to the long axes of the magnetite grains). For a suite of clay-rich magnetite-bearing sediments, we estimate $ARM_{\perp}/ARM_{||}$ by making a composite sample, giving it an inclined anhysteretic remanence and then applying a uniaxial compression and observing the change in remanence inclination and $ARM_{min}/ARM_{max}$. This estimated $ARM_{\perp}/ARM_{||}$ is used with the $ARM_{min}/ARM_{max}$ and $I$ from the natural specimens to estimate $I_{||}$, corrected for inclination shallowing. This method was shown to succeed for our three suites of clay-rich soft sediments bearing pseudo-single-domain magnetite: two from the continental rise off

Nova Scotia, Canada and one from the Shatsky Rise east of Japan. For compacted sediments with minimum ($K_{min}$) and maximum ($K_{max}$) magnetic susceptibility axes perpendicular and parallel to bedding respectively, theory also predicts (provided the magnetite grains are not single-domain) an approximately linear relation between $\tan I/\tan I_H$ and the susceptibility anisotropy parameter, $K_{min}/K_{max}$ (which is easier to measure than $ARM_{min}/ARM_{max}$). This relation was observed to hold for our composite samples during uniaxial compression experiments and was used to successfully estimate $I_H$, corrected for inclination shallowing.

Burial compaction can also reduce remanence intensity which can affect the sediment's record of paleointensity changes in the Earth's magnetic field. We observed an approximately linear relation between remanence intensity and the remanence anisotropy parameter $ARM_{min}/ARM_{max}$ during the uniaxial compression experiments on our composite samples. This is used to suggest a novel method of correcting for compaction-induced intensity decrease in magnetite-bearing soft sediments.

## ACKNOWLEDGEMENTS

This thesis is dedicated to my parents who have given me all manner of support and love while I have pursued my studies, without them I could never have completed this work.

My thesis advisor Dr. Joseph Hodych deserves more thanks than I could hope to express here. Thank you, Joe, for your encouragement, guidance and patience. I have been privileged to study in your lab. The research was supported by a research grant to Joseph Hodych from the Natural Sciences and Engineering Research Council of Canada. I also thank Dr. Charles Hurich who graciously served on my supervisory committee. I wish to thank my thesis examiners, Dr. Hugh Miller my internal examiner and Dr. Ken Buchan my external examiner. Their comments and suggestions were very insightful and much appreciated.

Thanks are also due Dr. Satria Bijaksana who did all the initial core sampling and measurements, paving the way for this research and on whose shoulders I stand to present this thesis.

All my friends, the old friends who have seen me through this project, the new friends I have met only recently, are all important to me and deserve many thanks for the fun times we've had and will continue to share, as well as the encouragement and understanding they have shown me. In particular, Michael Wheeler has been an invaluable labmate and (dare I say raillerious) friend, helping out during those many months we spent experimenting with and refining the techniques presented herein. Michael, don't forget -- 猿も木から落ちる!

## TABLE OF CONTENTS

Page

Page

## LIST OF TABLES

## LIST OF FIGURES

Page

Page

Page

## LIST OF ABBREVIATIONS AND SYMBOLS USED

*Abbreviations*

| | |
|---|---|
| AAR | Anisotropy of Anhysteretic Remanence |
| AF | Alternating Field |
| AGC | Atlantic Geoscience Centre |
| AMS | Anisotropy of Magnetic Susceptibility |
| ARM | Anhysteretic Remanent Magnetization |
| ChRM | Characteristic Remanent Magnetization |
| DC | Direct Current |
| DSDP | Deep Sea Drilling Project |
| GAD | Geocentric Axial Dipole |
| MD | Multi-domain |
| NRM | Natural Remanent Magnetization |
| PSD | Pseudo-single-domain |
| SD | Single-domain |
| SEM | Scanning Electron Microscope |
| SIRM | Saturation Isothermal Remanent Magnetization |

*Symbols*

| | |
|---|---|
| $ARM_{min}/ARM_{max}$ | The ratio of an intensity of an ARM applied along the hard axis of a sediment sample to that applied identically to the easy axis |

| | |
|---|---|
| $ARM_{\perp}/ARM_{\parallel}$ | The ratio of an intensity of an ARM applied perpendicular to the long axis of a magnetite particle to that applied identically parallel to the long axis |
| C | Slope of regression line on $\tan I/\tan I_H$ vs $K_{min}/K_{max}$ |
| B | Slope of regression line on $\tan I/\tan I_H$ vs $ARM_{min}/ARM_{max}$ |
| $H_c$ | Coercive force |
| $H_{cr}$ | Coercivity of remanence |
| $I$ | Inclination of Remanent Magnetization |
| $I_H$ | Inclination of Magnetizing Field |
| $J/J_o$ | Ratio of remanence intensity after compression to remanence intensity before compression |
| $J_{rs}$ | Saturation remanence |
| $K_{arm}$ | Anhysteretic susceptibility |
| $K_{mean}$ | Average magnetic susceptibility |
| $K_{min}$ | Magnetic susceptibility along a sample's hard axis |
| $K_{max}$ | Magnetic susceptibility along a sample's easy axis |
| $R$ | Pearson product moment coefficient of correlation |

# CHAPTER 1

# INTRODUCTION

## 1.1 Paleomagnetic Inclination Shallowing

Sedimentary rocks often possess a detrital remanent magnetization carried by magnetite grains. This remanence is acquired during sediment deposition or soon after, when the magnetic moments of the magnetite grains are preferentially aligned along the Earth's magnetic field direction.

It has long been known that the inclination of the natural remanence in sediments and sedimentary rocks can be significantly shallower than the inclination of the Earth's field at the time and location of their deposition, leading to underestimation of paleolatitude. This paleomagnetic inclination shallowing can have several causes (Butler, 1992) including errors occurring at the time of deposition (for example, due to grains rolling upon hitting the seafloor, especially in coarse-grained sediments) and errors occurring after deposition (for example, due to compaction upon burial of the sedimentary strata). For fine-grained clay-rich sediments, inclination shallowing can be especially large due to the large amount of compaction that these sediments undergo upon burial, before cementation. This compaction tends to rotate the long axes of magnetite grains towards the horizontal plane tending to decrease the inclination of remanence. This type of inclination shallowing has been the subject of much study and research (e.g. Jackson et al., 1991; Arason and Levi, 1990; Hodych et al., 1999; Deamer and Kodama, 1990).

As well as reducing remanence inclination, the compaction-induced rotation of the long axes of magnetite grains towards the horizontal plane also increases the anisotropy of the anhysteretic susceptibility of the sediments (Kodama and Sun, 1990). That is, it becomes harder to impart an anhysteretic remanence (ARM) perpendicular to the bedding plane of the sediments and easier parallel to bedding (since it is harder to magnetize perpendicular to the long axes of magnetite grains than parallel to their long axes). Several studies have attempted to make use of the relation between remanence inclination and ARM anisotropy to correct for inclination shallowing. For sediments with elongated magnetite grains obeying the long-axis distribution function of Stephenson et al. (1986), Jackson et al. (1991) derived a theoretical relation which Hodych and Bijaksana (1993) rewrote as:

$$\frac{\tan I}{\tan I_H} = \frac{\dfrac{\mathrm{ARM}_{min}}{\mathrm{ARM}_{max}} - 2\dfrac{\mathrm{ARM}_{\perp}}{\mathrm{ARM}_{||}} + \dfrac{\mathrm{ARM}_{min}}{\mathrm{ARM}_{max}} \times \dfrac{\mathrm{ARM}_{\perp}}{\mathrm{ARM}_{||}}}{1 - \dfrac{\mathrm{ARM}_{min}}{\mathrm{ARM}_{max}} \times \dfrac{\mathrm{ARM}_{\perp}}{\mathrm{ARM}_{||}}} \qquad (1.1)$$

$I$ is the remanence inclination observed in the sample and $I_H$ is the inclination of the Earth's magnetic field at the time that the sediment was deposited. $\mathrm{ARM}_{min}/\mathrm{ARM}_{max}$ is the ratio of intensities of ARM given identically along the sediment sample's hard and easy axes (which are assumed to lie perpendicular and parallel to the bedding plane respectively, with little anisotropy in the bedding plane) (Figure 1.1). $\mathrm{ARM}_{\perp}/\mathrm{ARM}_{||}$ is the average ratio of the intensities of ARM given identically perpendicular and parallel to the long axes of the individual magnetite grains in the sediment, which may be of any domain state but are assumed to be elongated enough

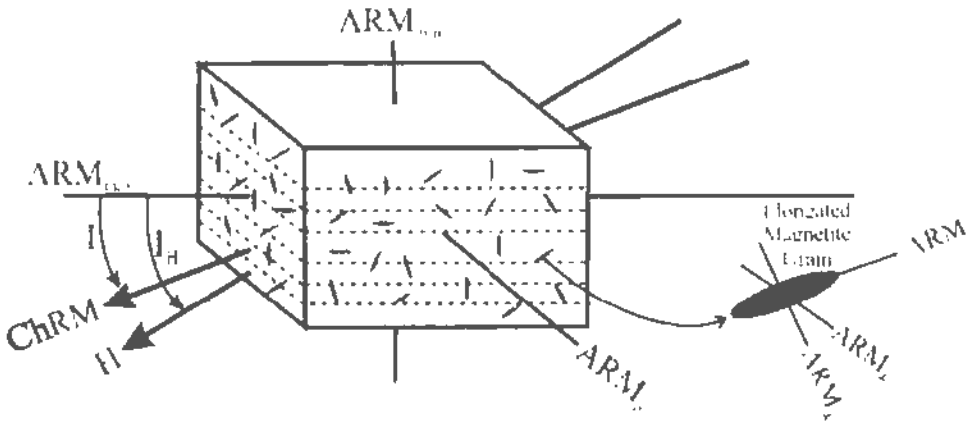


**Figure 1.1** A sediment with elongated magnetite particles (shown in grey above) that has undergone burial compaction is shown to have acquired remanence anisotropy with its hard axis ($ARM_{min}$) vertical – perpendicular to the horizontal bedding plane and with no anisotropy within the bedding plane. $I_H$ is the inclination of the earth's magnetic field during deposition of the sediment and $I$ is the inclination of the characteristic remanence (ChRM) after sediment compaction bas rotated the magnetite long axes towards the bedding plane, shallowing the inclination of the remanence. The average remanence anisotropy of the individual magnetite grains is characterized by $ARM_{\perp}/ARM$ which is the ratio of intensities of ARM given identically perpendicular and parallel to the long axes of the magnetite grains.

to be dominated by uniaxial shape anisotropy (Figure 1.1).

## 1.2 Correcting for Inclination Shallowing Using Magnetic Anisotropy

Relation 1.1 suggests that compaction-induced inclination shallowing can be corrected for, if the two anisotropy parameters $ARM_{min}/ARM_{max}$ and $ARM_{\perp}/ARM$ are known. While $ARM_{min}/ARM_{max}$ can be measured easily using oriented samples of the sediment, $ARM_{\perp}/ARM_{\parallel}$ is much more difficult measure.

Many attempts have been made to estimate $ARM_{\perp}/ARM$ by aligning magnetite particles (extracted from the sediment) in the presence of a magnetic field in a hardening medium like epoxy and measuring the ARM of the resulting bulk sample (e.g. Jackson et al, 1991; Bijaksana, 1996; Kodama, 1997; Tan and Kodama, 1998). Unfortunately, this method is problematic, often underestimating $ARM_{\perp}/ARM$ (Bijaksana, 1996; Tan and Kodama, 1998). This may be due to grain interaction between the magnetite particles in the presence of the strong magnetic field; the field not only aligns the long axes of the magnetite grains, but may also cause the grains to attract each other and form chains oriented along the magnetic field lines (Bijaksana, 1996, Hodych et al., 1999).

Another method of estimating $ARM_{\perp}/ARM$ is through artificially compacting a sample in the laboratory and monitoring the remanence inclination and remanence anisotropy change. A disaggregated sample of the sediment is mixed with water and deposited in the presence of a magnetic field to impart a detrital remanence. Then,

one measures how remanence inclination ($I$) and remanence anisotropy ($ARM_{min}/ARM_{max}$) change while water is forced out of the sediment as it is progressively compacted (Kodama, 1997; Tan and Kodama, 1998). The theory of Jackson et al. (1991) can then be used to determine $ARM_{\perp}/ARM$ for the sample. However, this method can be difficult and time-consuming (Hodych and Bijaksana, 1993).

Hodych and Bijaksana (1993) pointed out that it may be possible to correct for inclination shallowing without measuring $ARM_{\perp}/ARM$. They showed that relation 1.1 predicts a roughly linear correlation between tan$I$ and $ARM_{min}/ARM_{max}$ (as shown in Figure 1.2). Hodych et al. (1999) found such a correlation between tan$I$ and $ARM_{min}/ARM_{max}$ in a suite of magnetite-bearing sediment samples and used it to extrapolate to $ARM_{min}/ARM_{max} = 0$ to successfully estimate $I_H$ (Figure 1.3a). Hodych et al. (1999) also showed that a linear correlation between tan$I$ and the susceptibility anisotropy parameter ($K_{min}/K_{max}$) is expected, provided that the magnetite grains are not single-domain. This linear correlation between tan$I$ and $K_{min}/K_{max}$ was found to be equally successful in predicting $I_H$ (Figure 1.3b) for a suite of clay-rich sediments bearing pseudo-single-domain magnetite, and was much faster to measure. This method is not always applicable because it requires that the specimens in the suite of samples have a large enough variation in $ARM_{min}/ARM_{max}$ (or $K_{min}/K_{max}$) to yield a statistically significant correlation. Hence it remains desirable to have a simple method for estimating the anisotropy parameter $ARM_{\perp}/ARM$ of the magnetite

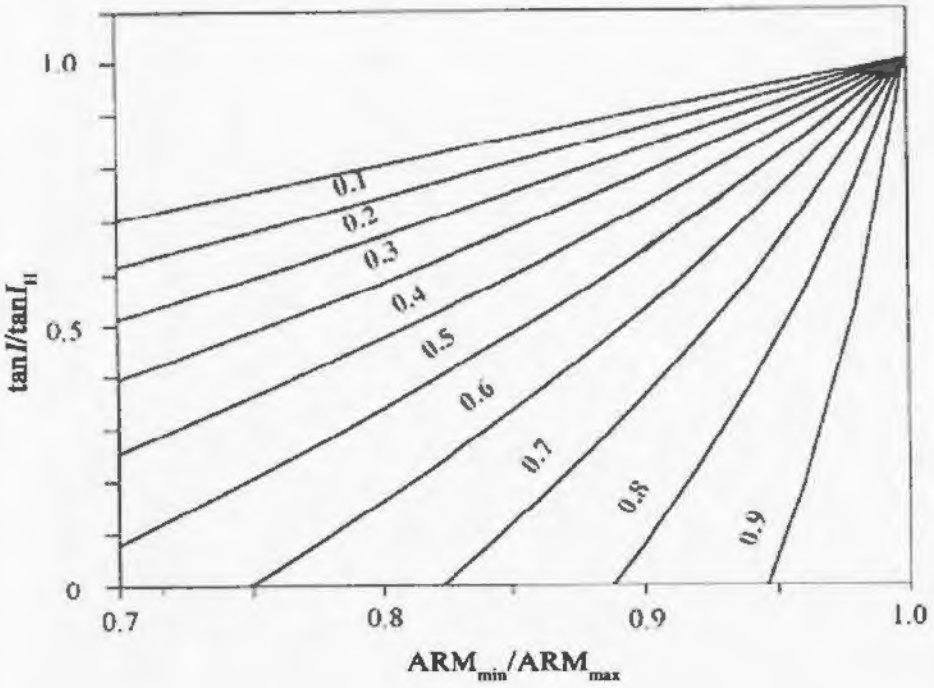


**Figure 1.2** The theoretical relation predicted for compacted sediment by Equation 1.1 between tan$I$/tan$I_H$ and $ARM_{min}/ARM_{max}$ for various values of magnetite particle anisotropy parameter $ARM_{\perp}/ARM_{\parallel}$. Uncompacted sediment should begin with tan$I$/tan$I_H$ = 1 (no inclination shallowing) and $ARM_{min}/ARM_{max}$ = 1 (no anisotropy). During compaction, the samples should move down along one of the curves whose slope depends upon the average anisotropy parameter $ARM_{\perp}/ARM_{\parallel}$ of the individual magnetite grains.

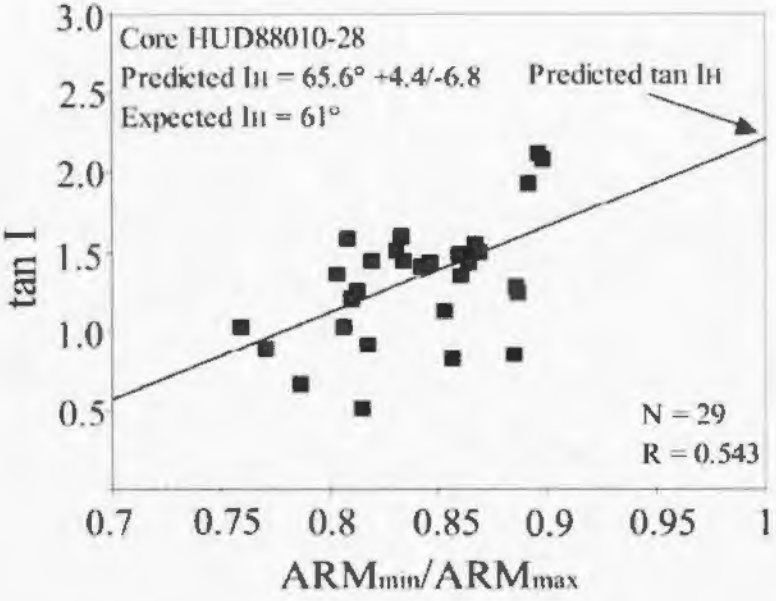


(a)

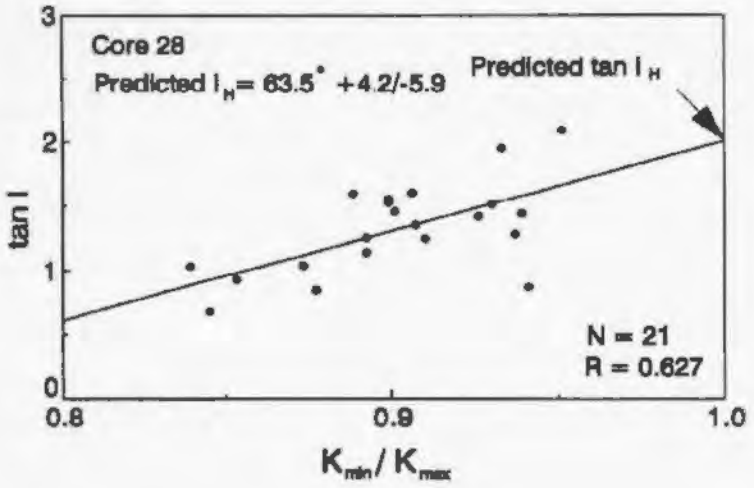


(b)

**Figure 1.3 (a)** Using the linear correlation between tan*I* and ARMmin/ARMmax to estimate $I_H$ **(b)** Using the linear correlation between tan*I* and $K_{min}/K_{max}$ to estimate $I_H$ (from Hodych et al., 1999; N is tbe number of samples and R is the Pearson product moment correlation coefficient, see Appendix E).

particles.

Hodych and Bijaksana (2002) explored a novel approach for estimating magnetite particle anisotropy ($ARM_{\perp}/ARM_{\parallel}$) by plastically deforming a magnetite-bearing clay-rich sediment sample using axial compression. They repeatedly compressed the sample until its remanence anisotropy reached a saturation level. They assumed that repeated compression forced the rotation of all the (elongated) magnetite grains into the horizontal plane (perpendicular to the compression axis) thus allowing estimation of $ARM_{\perp}/ARM_{\parallel}$ by comparing the ease of giving ARM perpendicular and parallel to the horizontal plane of the compressed sample. However, the remanence anisotropy of the compressed sample yielded an overestimate of $ARM_{\perp}/ARM_{\parallel}$ suggesting that the long axes of the grains were not all completely rotated into the horizontal plane. This failed approach led Hodych and Bijaksana (2002) to try a modification which proved promising and is the method explored in detail in the present thesis.

## 1.3 Objectives of This Study

The anisotropy parameter ($ARM_{\perp}/ARM_{\parallel}$) of the magnetite particles in a suite of magnetite-bearing clay-rich specimens is estimated by making up a composite sample and kneading it to randomize the long axes of the magnetite grains. The composite sample is given an inclined remanence (an ARM) and is then compressed along a vertical axis. This plastically deforms the sample, causing the magnetite long

axes to rotate towards the horizontal plane. This reduces remanence inclination and induces a magnetic anisotropy with hard axis vertical and little anisotropy in the horizontal plane. The remanence inclination (*I*) after compression and the anisotropy parameter $ARM_{min}/ARM_{max}$ of the composite sample are measured and substituted into Equation 1.1 allowing an estimate of average $ARM_{\perp}/ARM$ . This can then be used in Equation 1.1 to correct for shallowing of the natural remanence in each of the specimens in tbe suite. This simple method is shown to successfully correct for inclination shallowing in the three piston cores of clay-rich magnetite-bearing sediments studied. This method is similar to that used by Deamer and Kodama (1990) and Tan and Kodama (1998) but uses laboratory *compression* rather than time-consuming laboratory *compaction* to model the burial compaction of magnetite-bearing clay-rich sediments.

This thesis also explores how susceptibility anisotropy changes as laboratory compression reduces remanence inclination in the composite samples. This leads to a new method of using natural susceptibility anisotropy to correct for inclination of natural remanence in a suite of clay-rich magnetite-bearing specimens provided that the magnetite is not single-domain.

Finally we show that compression very significantly reduces remanence intensity and we suggest a method of using magnetic anisotropy to correct for this effect in paleointensity studies using magnetite-bearing soft sediment piston cores.

# CHAPTER 2

# SAMPLE DESCRIPTIONS

## 2.1 Sample Description and Rock Magnetic Properties

The marine sediments used in this study were studied paleomagnetically by Bijaksana (1996). Two sets of turbidite mud samples were obtained from the Atlantic Geoscience Centre from piston cores HUD88010-28 and HUD88010-24 (to be called Core 28 and Core 24 in this thesis). These cores were collected from the continental rise south of Nova Scotia, Canada (Figure 2.1). These specimens were clay-rich as shown for specimens from Core 28 which contained ~27% illite and ~22% kaolinite according to X-ray diffraction analysis (Hodych et al., 1999). Specimens from a piston core in pelagic mud (DSDP Site 578) from the Shatsky Rise approximately 1000 km east of Japan (Figure 2.2) were also used in the current study. These specimens were even more clay-rich, containing as much as 93% clay by weight in some parts of the core (Bijaksana, 1996).

Bijaksana (1996) showed that the cores studied were dominated by magnetite judging by the Curie points. For cores 24 and 28, he measured susceptibility of seven typical samples (five from Core 28 and two from Core 24) as a function of high temperature to determine Curie points of ~580°C, indicating dominance by pure magnetite (Figure 2.3a). For Site 578, five typical samples yielded a dominant Curie point near 510°C as well as a less pronounced Curie point near 580°C suggesting

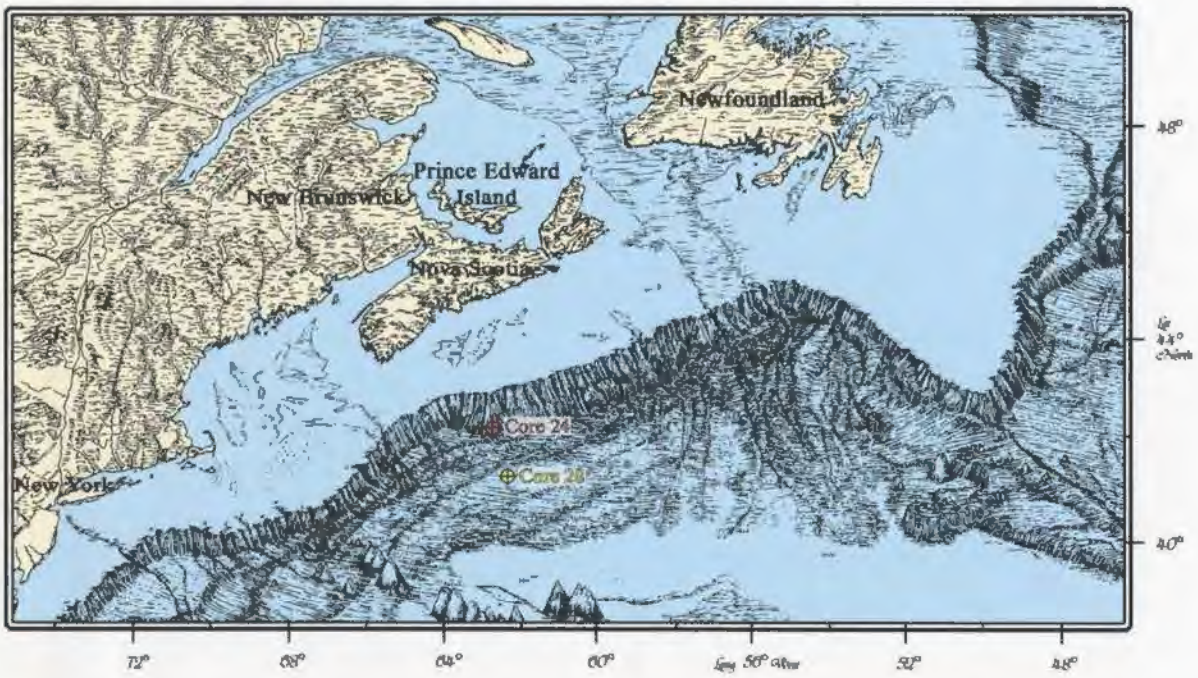


**Figure 2.1** Piston core sites on the Scotian Rise where cores 28 and 24 were obtained (stored at the Atlantic Geosciences Centre) and described by Berry and Piper (1993) as distal turbidites.

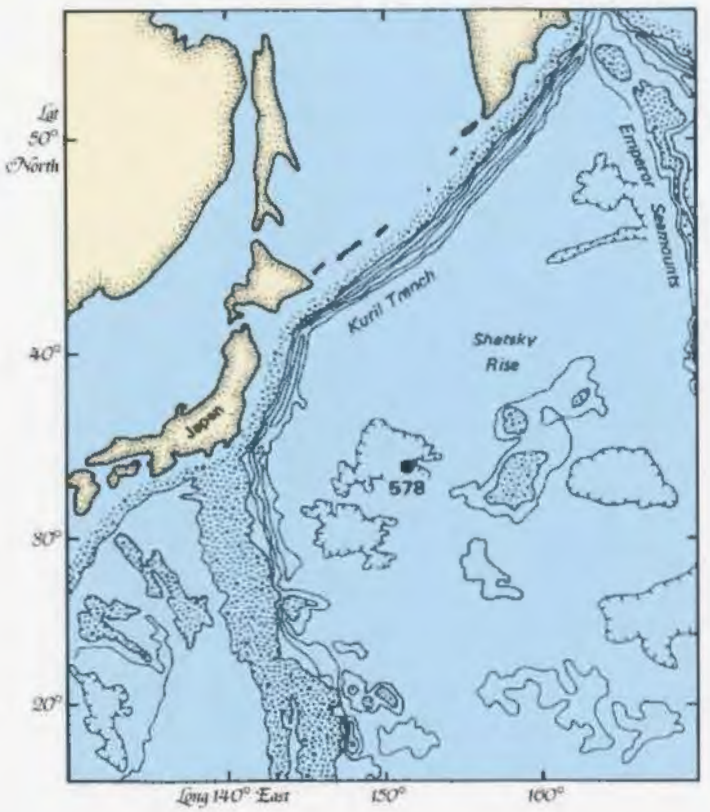


**Figure 2.2** Location map of DSDP piston core Site 578, off the coast of Japan.

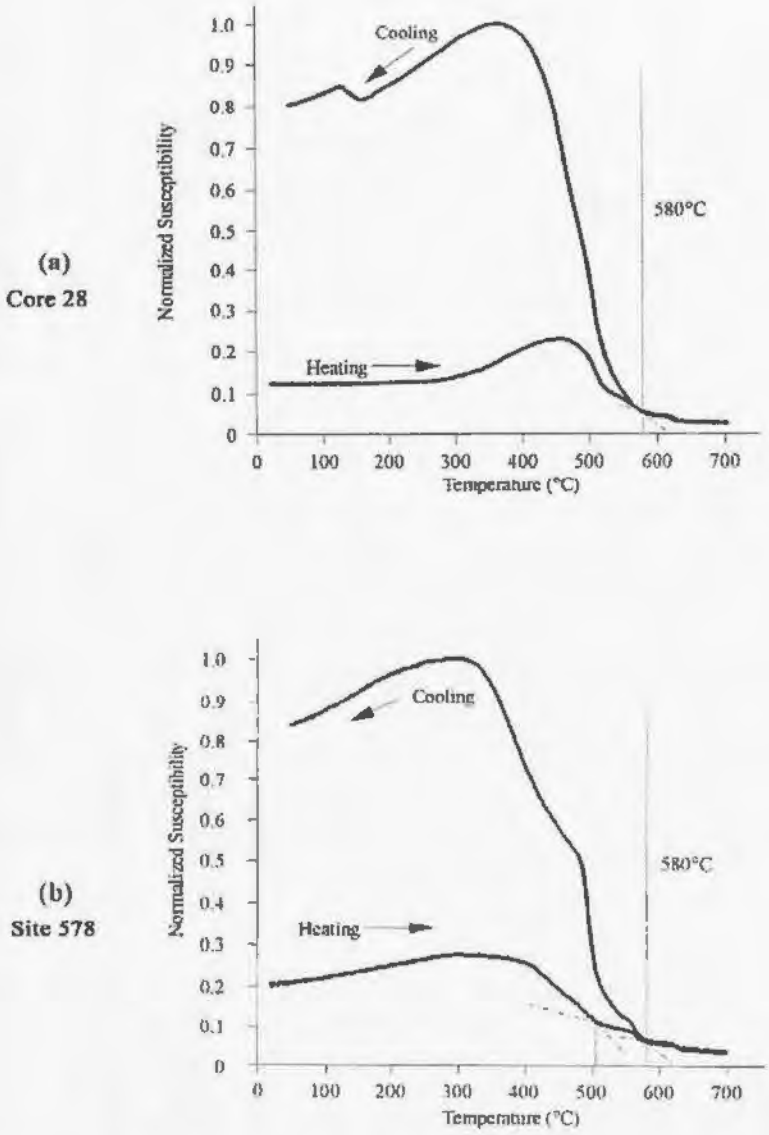


**Figure 2.3** **(a)** Normalized magnetic susceptibility of a typical turbidite specimen (28-0714) from the Scotian Rise (Core 28, 7.14 meters below the seafloor) as a function of temperature. A rise of susceptibility as the Curie point is approached indicates the Hopkins effect. The decline of susceptibility at 580°C suggests the presence of pure magnetite. **(b)** Normalized susceptibility of a typical pelagic clay specimen from Site 578 (35.92 meters below the seafloor) as a function of temperature. On heating, the main magnetic mineral shows a Curie point of about 510°C suggesting magnetite with a small titanium content. A smaller amount of pure magnetite also seems to be present as indicated by its Curie point of about 580°C. (Both diagrams are from Bijaksana, 1996).

dominance by magnetite with a small titanium content as well as the presence of a smaller amount of pure magnetite (Figure 2.3b).

Bijaksana used hysteresis properties measured for each specimen to show that the magnetite was likely dominantly pseudo-single-domain. That is, hysteresis loops for each specimen were obtained, giving coercive force ($H_c$), saturation magnetization ($J_s$) and saturation remanence ($J_{rs}$). Coercivity of remanence ($H_{cr}$) was also determined and $J_{rs}/J_s$ vs $H_{cr}/H_c$ was plotted (Figure 2.4) following Day et al. (1977). Semi-quantitative scanning electron microscope (SEM) energy dispersive X-ray analyses were obtained for individual grains in a magnetic extract from composite samples of cores 24 and 28 and showed that the weight ratio of $TiO_2$/FeO averages $0.01 \pm 0.02$ for cores 28 and $0.01 \pm 0.01$ for Core 24, indicating a very low titanium content and essentially pure magnetite. In contrast, the magnetic extract from Site 578 was shown to have a weight ratio of $TiO_2$/FeO of approximately 0.4, which indicates a high titanium content, suggesting that the magnetite grains at Site 578 contain ilmenite exsolution lamellae too fine to see within the magnetite grains. Representative SEM micrographs of magnetic extracts from of each of the cores studied are shown in Figure 2.5.

## 2.2 Paleomagnetic and Magnetic Anisotropy Measurements of Bijaksana

Bijaksana (1996) obtained each of the specimens used by pushing a cylindrical sleeve of plastic of 22 mm internal diameter and19 mm length into the piston core

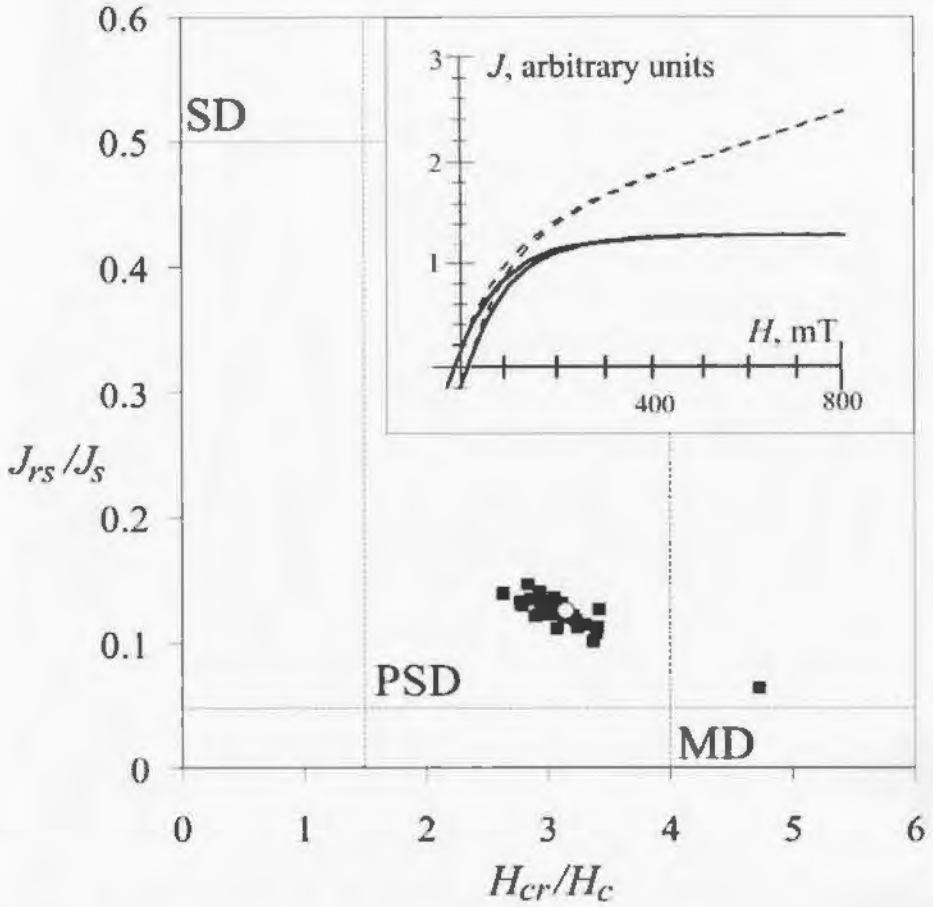


**Figure 2.4** The ratio $J_{rs}/J_s$ of saturation remanence to saturation magnetization plotted against the ratio $H_{cr}/H_c$ of coercivity of remanence to coercive force for 29 specimens of Core 28. The single-domain, pseudo-single-domain and multidomain fields are indicated by SD, PSD and MD respectively following Day et al. (1977). The open circle denotes a typical sample whose hysteresis loop is shown before (dashed line) and after (solid line) correcting for a paramagnetic contribution to the magnetization $J$ in a magnetic field $H$ (from Hodych and Bijaksana, 2002).

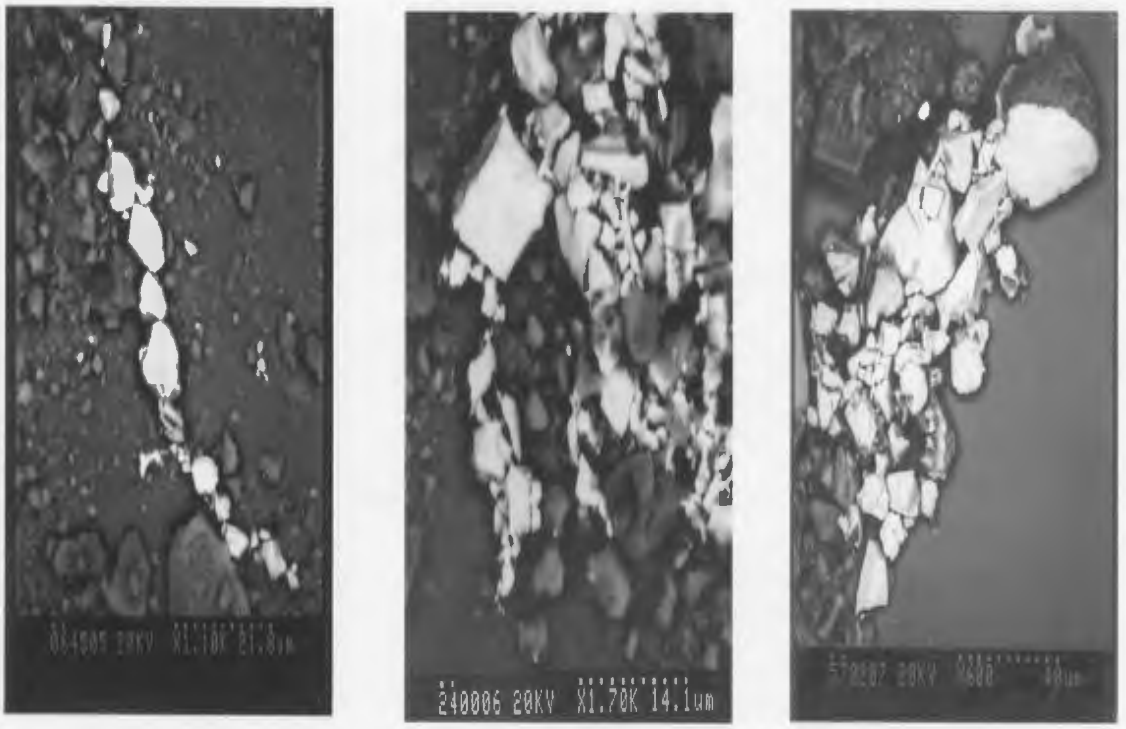


Core 28 Core 24 Site 578

Figure 2.5 Scanning electron microscope (SEM) backscattered images of magnetite grains (which appear bright) magnetically extracted from a specimen of core 28, core 24, and site 578.

perpendicular to the core's axis (Figure 2.6). The core's azimuth was not known. The cores were studied paleomagnetically by Bijaksana (1996) and exhibited a relatively high degree of inclination shallowing. On average, characteristic remanent magnetization (ChRM) was shallower than expected from the geocentric axial dipole (GAD) model by 8.7° for Core 28, 7.3° for Core 24 and 4.6° for Site 578.

The characteristic remanent magnetization (ChRM) of each specimen was measured by Bijaksana (1996) using a CTF Systems Inc. superconducting magnetometer or a Schonstedt spinner magnetometer (model SSM-1), the former for specimens with weaker remanence and the latter for specimens with stronger remanence. In measuring the characteristic remanence of a specimen, one aims to isolate the primary component of remanence (the magnetization acquired during deposition of the sediment) from the secondary component of remanence (the magnetization that may have been acquired in the intervening geologic time). Because the primary component is usually magnetically more stable than the secondary component, it is possible to preferentially remove the secondary remanence and isolate the primary remanence during detailed stepwise demagnetization.

Each specimen was demagnetized in a Schonstedt demagnetizer (model GDS-1, Figure 2.7b) using stepwise alternating field demagnetization, starting with a peak alternating field of 5 mT increasing by steps of 5 mT up to 40 mT, whereupon the

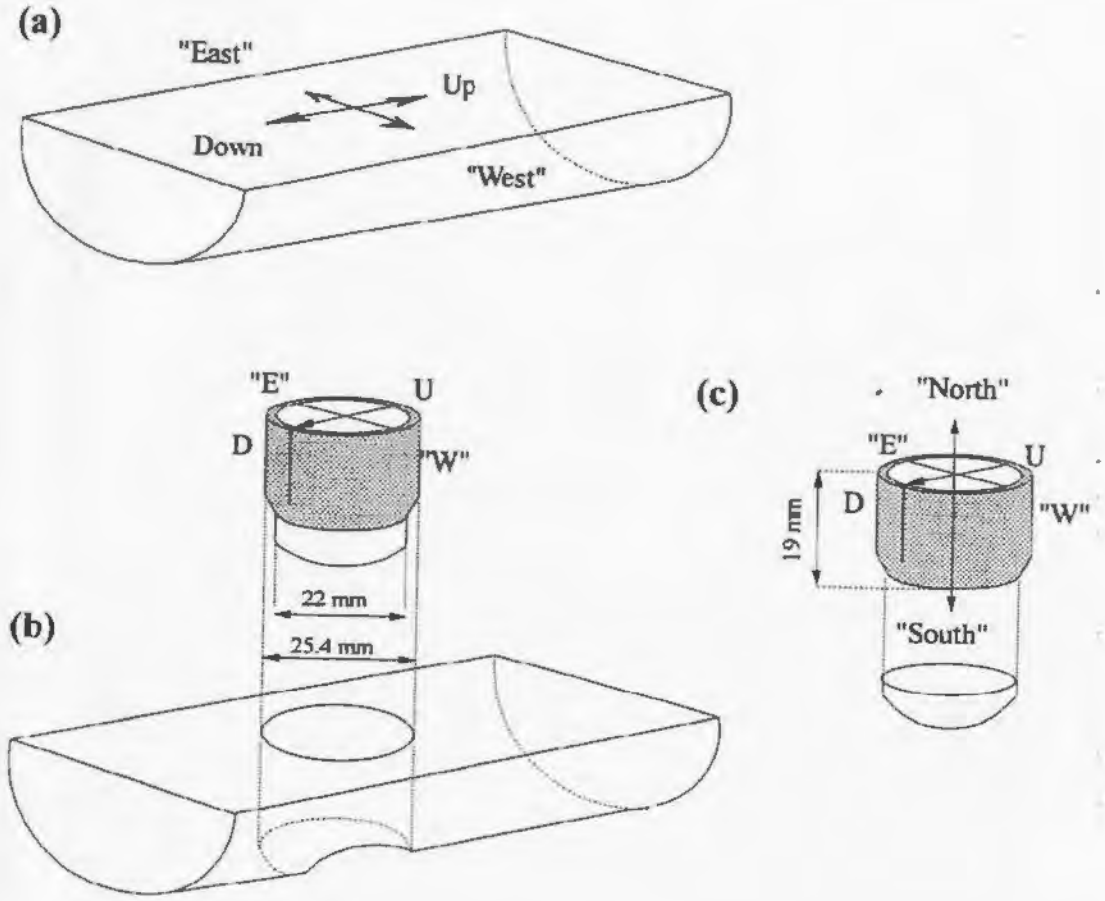


**Figure 2.6** Schematic diagram of the sampling technique employed by Bijaksana (1996). **(a)** The vertical and horizontal orientations are marked on the split core sample. **(b)** A tapered cylindrical plastic holder is then pushed into the core using a mechanical press (not drawn) that was designed to prevent holder rotation during penetration. The holder is also marked for down and up orientations. **(c)** The specimen is then trimmed to fit the holder. Note that the 'east-west' and the 'north-south' axes are arbitrary (Bijaksana, 1996).

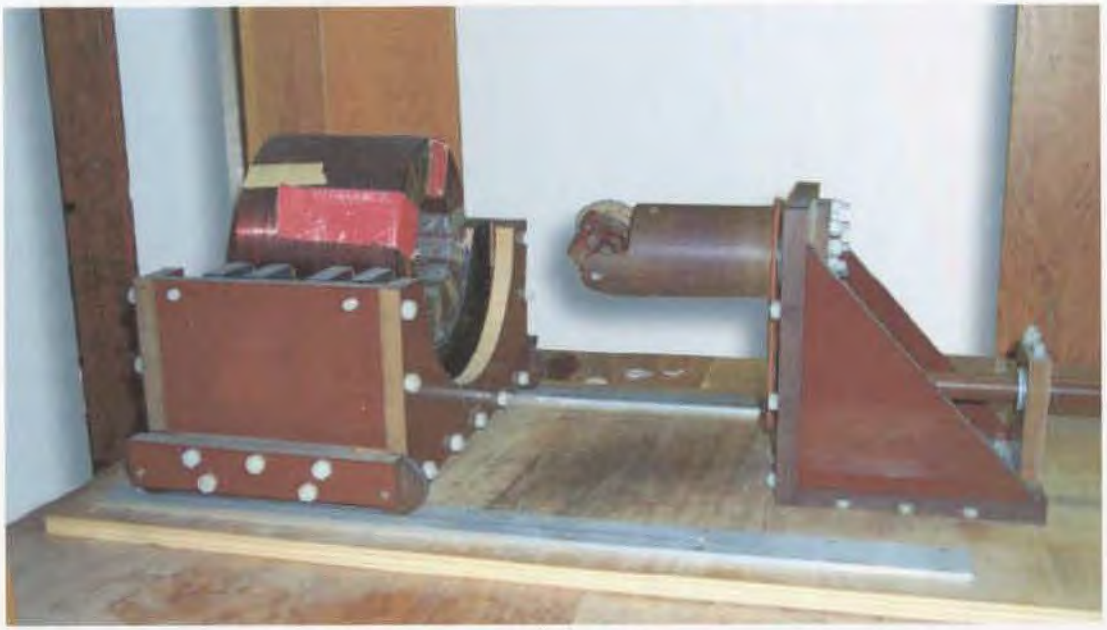

(a)

(b)

**Figure 2.7 (a)** The three-axis tumble demagnetizer used in the present study. **(b)** Schonstedt model GDS-1 alternating field demagnetizer. (Note the switchbox in front of the demagnetizers that controls the DC field.)

steps were increased to 10mT up to a final peak field of 100mT or until the remanence decreased to less than 10% of its original intensity (Bijaksana, 1996). The characteristic remanent magnetization direction (the best estimate of the primary magnetization direction) was determined by Bijaksana (1996) using a computer program that performs principal component analysis (Kirschvink, 1980). Typical intensity decay plots and vector plots (well described by Butler, 1992) are given in Figures 2.8.

For the experiments described in this thesis, we chose those of Bijaksana's specimens that had stable remanence and whose hard axis ($ARM_{min}$) was within 15° of vertical. The paleomagnetic results for the specimens used are listed in Appendix A and summarized in the following table:

**Table 2.1** Summary of the average paleomagnetic and rock magnetic properties of specimens collected by Bijaksana (1996) and used in the current study as presented in detail in Appendix A.

| Sample | $I_H$ (°) GAD | $I$ (°) ChRM | $ARM_{min}$/ $ARM_{max}$ | $K_{min}/K_{max}$ |
|---|---|---|---|---|
| Core 28 | 60.6 | 51.4 ± 3.2 | 0.839 | 0.902 |
| Core 24 | 61.1 | 53.8 ± 4.5 | 0.859 | 0.918 |
| Site 578 | 53.4 | 48.8 ± 3.7 | 0.961 | 0.980 |

The second column gives $I_H$, the inclination of remanence expected from the geocentric axial dipole (GAD) model. The third column gives the average inclination of the characteristic remanence $I$. The fourth column gives the average remanence anisotropy parameter $ARM_{min}/ARM_{max}$ and the last column gives the magnetic susceptibility anisotropy parameter $K_{min}/K_{max}$.

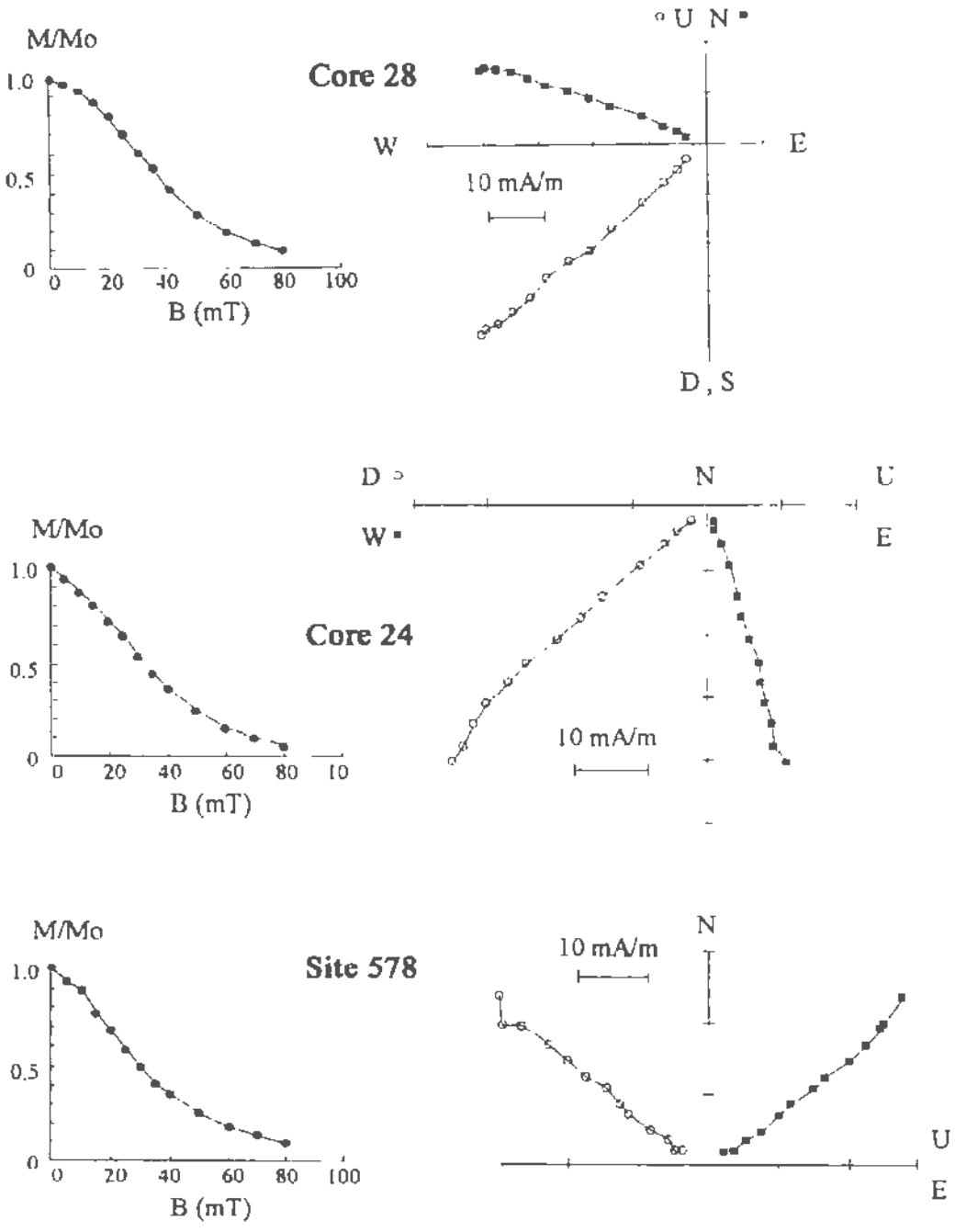


**Figure 2.8** Typical intensity decay curves and vector plots of the components of the natural remanence (NRM) during AF demagnetization for representative turbidite specimens of cores 28 and 24 and Site 578 showing a stable characteristic remanence that decays steadily with increasing alternating field demagnetization (Bijaksana, 1996).

## 2.3 Remanence Anisotropy in the Natural Specimens

The anisotropy of anhysteretic remanence (AAR) was measured and described by Bijaksana (1996) for each of his specimens for which ChRM was determined. After demagnetization in an alternating field of least 70 mT, the specimen was placed in the Schonstedt alternating field demagnetizer and a 70 mT alternating field was reduced to zero in the presence of a 0.2 mT magnetic field, both applied to the specimen's vertical axis (U-D) giving this axis an anhysteretic remanent magnetization (ARM). The 0.2 mT field was generated by passing a direct current from a 12-volt battery through turns of wire wound around the outside of the demagnetizer coil, with a large self-inductance in the circuit to minimize any current induced by the alternating field (Figure 2.7b).

Bijaksana (1996) gave each of his natural specimens an ARM in this way along nine directions (U-D, N-S, E-W, NE-SW, ND-SU, ED-WU, NW-SE, NU-SD and EU-WD) measuring and demagnetizing before giving the next ARM. This was repeated in the opposite sense for each of the nine directions to average out any remanence not removed in demagnetization. The nine pairs of measurements allowed the full anhysteretic remanence anisotropy tensor to be determined and the intensity and direction of the three principal axes of AAR ($ARM_{min}$, $ARM_{int}$ and $ARM_{max}$) were listed by Bijaksana (1996) for each of his specimens. The remanence anisotropy parameter $ARM_{min}/ARM_{max}$ is listed in Appendix A for each specimen we used. Each specimen has $ARM_{min}$ within 15° of vertical and $ARM_{int} \approx ARM_{max}$.

## 2.4 Susceptibility Anisotropy of the Natural Specimens

Anisotropy of magnetic susceptibility (AMS) was measured for each natural specimen by Bijaksana (1996) using a Sapphire Instruments (model SI2B. Figure 2.9) magnetic susceptibility meter. Since these measurements were made after AAR measurements, the specimens were demagnetized using 3-axis tumble demagnetization with a peak field of 100 mT prior to AMS measurement to avoid field-impressed susceptibility anisotropy (Bijaksana, 1996).

Magnetic susceptibility was measured along six different orientations: N-S, NE-SW, E-W, D-U, ND-SU, ED-WU. The specimen was measured in the two opposite directions for each orientation giving a total of 12 measurements. A computer program provided with the instrument uses these measurements to estimate the magnitudes and directions of the three principal susceptibility axes $K_{min}$, $K_{int}$ and $K_{max}$ of the susceptibility anisotropy tensor and these were listed by Bijaksana (1996) for each natural specimen. The susceptibility anisotropy parameter $K_{min}/K_{max}$ is listed in Appendix A for each specimen used (each of these specimens has $K_{min}$ within 15° of vertical and $K_{int} \approx K_{max}$).

## 2.5 The Composite Samples Used in the Compression Experiments

For each piston core, a composite sample was prepared for compression experiments by using a small amount of sediment from each of the natural specimens from the core (i.e. with stable remanence and with $ARM_{min}$ within 15° of vertical).

**Figure 2.9** Sapphire Instruments (model SI2B) magnetic susceptibility meter. (Note the sample in the plastic holder in front of the instrument.)

More details of sample preparation are given in section **3.1**.

## 2.6 Susceptibility Anisotropy of the Composite Samples

The susceptibility anisotropy parameter $K_{min}/K_{max}$ of the composite sample used in the compression experiments was also measured using a Sapphire Instruments (model SI2B, Figure 2.9) magnetic susceptibility meter. As with the natural specimens the composite sample was measured along the six orientations: N-S, NE-SW, E-W, D-U, ND-SU, ED-WU. The composite sample was also measured in the two opposite directions for each orientation giving a total of 12 measurements. A computer program provided with the instrument uses these measurements to estimate the magnitudes and directions of the three principal susceptibility axes $K_{min}$, $K_{int}$ and $K_{max}$ of the susceptibility anisotropy tensor. The susceptibility anisotropy parameter was calculated by dividing the $K_{min}$ by the $K_{max}$ value, and is listed in Appendix B.

## 2.7 Remanence Anisotropy of the Composite Samples

In measuring the remanence anisotropy parameter $ARM_{min}/ARM_{max}$ of the composite samples used in the compression experiments, the full tensor was not determined. Since the susceptibility anisotropy tensor showed that $K_{min}$ was always within 5E of vertical and that $K_{int} \approx K_{max}$, to save time, it was assumed that $ARM_{min}$ was vertical and that $ARM_{int}$ was also approximately equal to $ARM_{max}$ in measuring $ARM_{min}/ARM_{max}$. To do this, an anhysteretic remanence was applied (in the same

way as used by Bijaksana (1996) and described above) and measured along the three orthogonal directions (N-S, E-W and U-D) and the reverse, demagnetizing between steps. The two ARM measurements along the U-D axis were averaged to give an estimate of $ARM_{min}$. After checking that the two ARM measurements along the N-S axis did not differ significantly (<2% difference) from the two ARM measurements along the E-W axis, these four measurements were averaged to give an estimate of $ARM_{max}$. The ratio of these $ARM_{min}$ to $ARM_{max}$ estimates were then listed (Appendix B) and used.

# CHAPTER 3

## MEASURING THE EFFECT OF AXIAL COMPRESSION UPON REMANENCE INCLINATION AND MAGNETIC ANISOTROPY OF THE COMPOSITE SAMPLES

### 3.1 Sample Preparation and Compression Experiments

For each core, a composite sample was prepared using a small amount of sediment from each of the samples that had stable remanence and $ARM_{min}$ axis within 15° of vertical (listed in Appendix A). This sediment was kneaded together with water and then formed by hand into a 2.2 cm diameter sphere. The sphere was slightly compressed in a non-magnetic hand press (Figure 3.1) to shape it, giving it six flat faces, like a cube with rounded edges. This was done to help maintain the sample's correct up-down (U-D) orientation, (i.e., to prevent the sample from rotating during later compression). To ensure that the sample's original north-south (N-S) axis remained correctly oriented during the experiments, the down face of the sample was marked with a north-directed arrow using a felt-tipped pen.

The sample was then placed in a small plastic 2 cm cubic holder and tumble demagnetized (Figure 2.7a) in a peak alternating field of 100 mT. The sample holder was lined with a thin removable acetate liner to facilitate extraction of the sample without deforming it. The anisotropy of magnetic susceptibility (AMS) was measured to confirm that the susceptibility of the sample was isotropic (AMS < 2%) indicating that the long axes of the magnetic grains were approximately

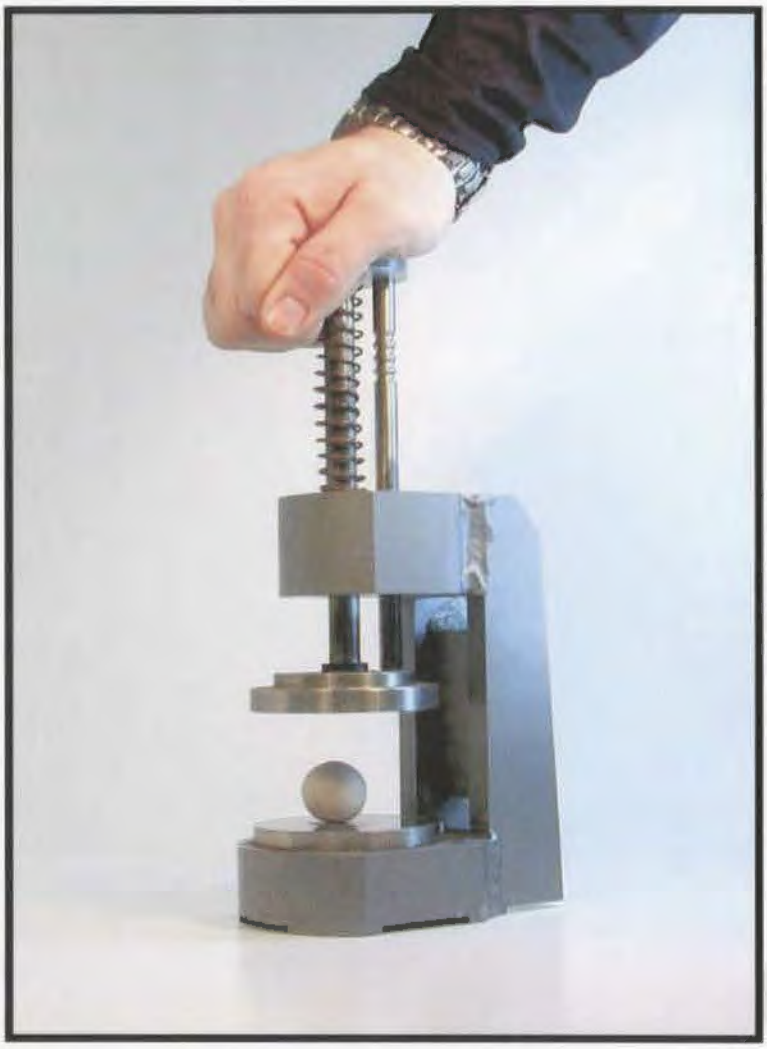

**Figure 3.1** The non-magnetic press used to plastically deform sediment samples.

randomly oriented. The magnetic susceptibility anisotropy parameter, $K_{min}/K_{max}$, was accurately measured using a Sapphire Instruments magnetic susceptibility meter (model SI2B, Figure 2.9) with a 12 orientation measurement (as described is section 2.6). The values and orientations of $K_{min}$, $K_{int}$ and $K_{max}$ were determined and checked to ensure that they did not differ by more than ~2%. If AMS was observed to be greater than 2% the sample was removed from the holder and the above process was repeated until AMS < 2% was achieved.

The remanence anisotropy ($ARM_{min}/ARM_{max}$) of the sample was measured (as described in section 2.7), and then the sample was tumble demagnetized in an alternating field of at least 100 mT. The sample was then given an inclined ARM by placing it in a Schonstedt demagnetizer (model GSD-1, Figure 2.7b). A 0.2 mT DC magnetic field was applied while a 70 mT (700 Oe) coaxial alternating field was reduced to zero. A special holder held the sample at a ~60° inclination to the applied field axis resulting in an anhysteretic remanence in the sample with an inclination of ~60° to the U-D axis. The inclination and intensity of this ARM was accurately measured using a Schonstedt spinner magnetometer (model SSM-1). Once the sample had been prepared in this way for compression experiments, it was subjected to a single-step compression experiment or a four-step incremental compression experiment.

## 3.2 Single-Step Compression Technique

In the single-step compression experiments, the spherical sample (with flattened faces, randomized magnetic grains and ~60° inclination ARM) was removed from the holder and its liner. It was then compressed in one step along the up-down axis to a disk of either 1.0 cm or 0.5 cm thickness in a non-magnetic press. The resulting sample disk was either trimmed to fit into the holder or cut into quadrants and stacked into the holder. In trimming, the disk was trimmed to a 2 cm square and placed in the plastic holder with polystyrene spacers to centre it vertically (Figure 3.2). In stacking (which can only be performed for full compression to 0.5 cm), the disk was cut into four quadrants, which were stacked into the holder in a way that avoided a preferred orientation of the magnetite long axes in the horizontal plane (Figure 3.3).

The north-directed arrow on the Down face of the sample was used to ensure that the sample was oriented properly. Measurements of the remanence inclination and intensity, and of $ARM_{min}/ARM_{max}$ and/or $K_{min}/K_{max}$ were repeated on the trimmed or stacked disks after compression. After the single-step compression experiments, the clay was kneaded to randomize the grains, given an inclined ARM and the experiment was repeated. There was no significant difference notieed between the results of the two methods of preparing the disks but trimming was more versatile, allowing incremental compression experiments. The results of all the single-step compression experiments are listed in Appendix B.

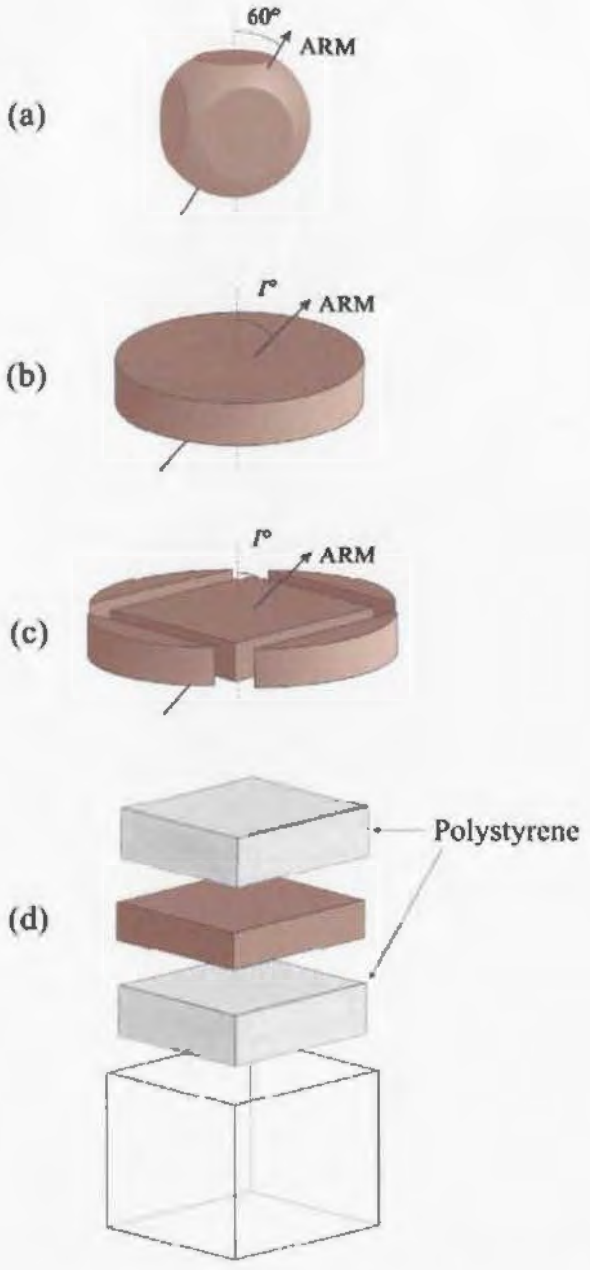


**Figure 3.2 (a)** The composite sample is kneaded to randomize the magnetic grains, shaped into a sphere, given flat faces and then and given an inclined ARM ($I \approx 60°$). **(b)** Compressing the sample produces a disk of a certain thickness depending on the size of spacer used. **(c)** The disk is trimmed to 2 cm on a side to fit into the 2 cm cubic holder. **(d)** The sample is centered vertically using polystyrene spacers and magnetic measurements are made. The sample is then removed and either compressed further or reassembled to produce a sphere as in (a), etc.

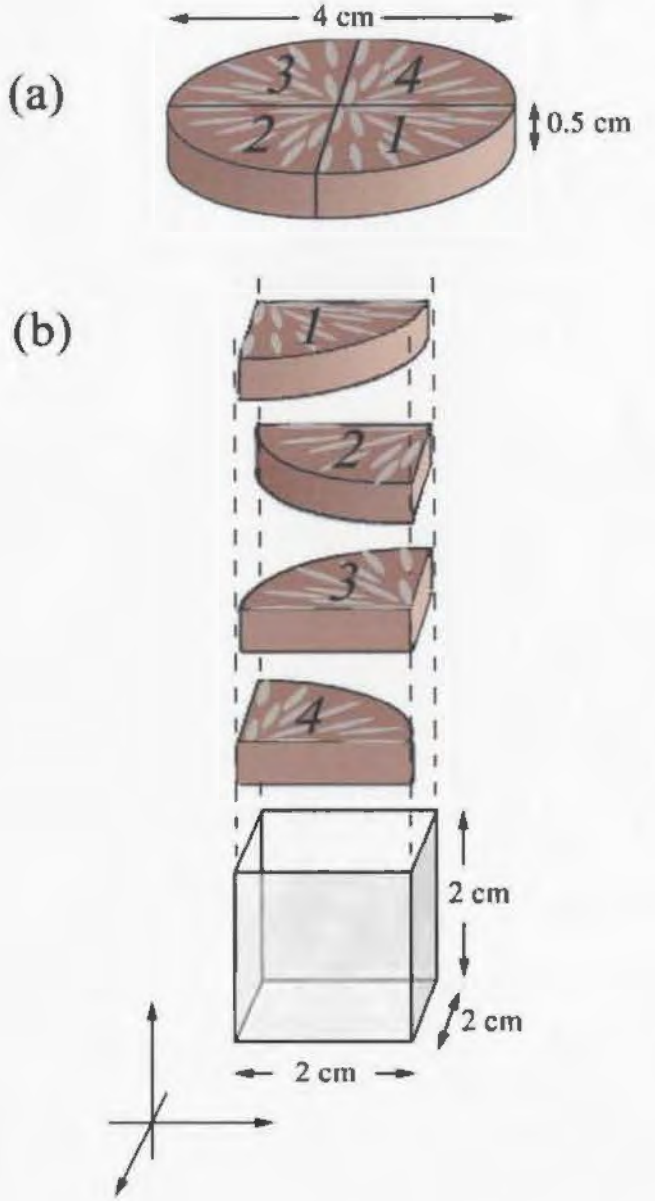


**Figure 3.3 (a)** Compressing the composite sediment sample produces a 4 cm diameter disk of 0.5 cm thickness (full compression). **(b)** The disk is cut into quadrants and stacked into a cubic holder for magnetic measurements.

### 3.3 Four-Step Incremental Compression Technique

Four-step incremental compression was used to save time in measuring the effect of compression upon ARM inclination and $K_{min}/K_{max}$ (but not $ARM_{min}/ARM_{max}$). In these incremental experiments, the spherical composite sample (with flattened faces, randomized magnetic grains and ~60° inclination ARM) was removed from the holder and liner and compressed using the non-magnetic press of Figure 3.1. It was first compressed to a 1.625 cm thick disk which was trimmed to fit into the 2 cm cubic holder (as in Figure 3.2). Once the trimmed sample was placed in the holder with north-directed arrow properly oriented, the ARM inclination and intensity were measured, and then $K_{min}/K_{max}$ was measured as described in section 2.6. ($ARM_{min}/ARM_{max}$ was not measured to avoid destroying the inclined ARM and having to knead the sample again and give it a new ARM of 60° inclination.)

The trimmed 1.625 cm thick sample was then compressed to 1.250 cm thickness and trimmed to fit the 2 cm cubic holder and the ARM inclination and intensity and $K_{min}/K_{max}$ were measured again. The trimmed 1.250 cm thick sample was then compressed to 0.875 cm, trimmed and measured. Finally, the trimmed 0.875 cm thick sample was compressed to 0.500 cm thickness and trimmed and measured. After these four steps of incrementally compressing (Figure 3.4), trimming and measuring of ARM inclination and intensity and $K_{min}/K_{max}$, the clay was reassembled and kneaded into a 2.2 cm diameter sphere and the set of experiments

was repeated. The results of these four-step incremental compression experiments are listed in Appendix B.

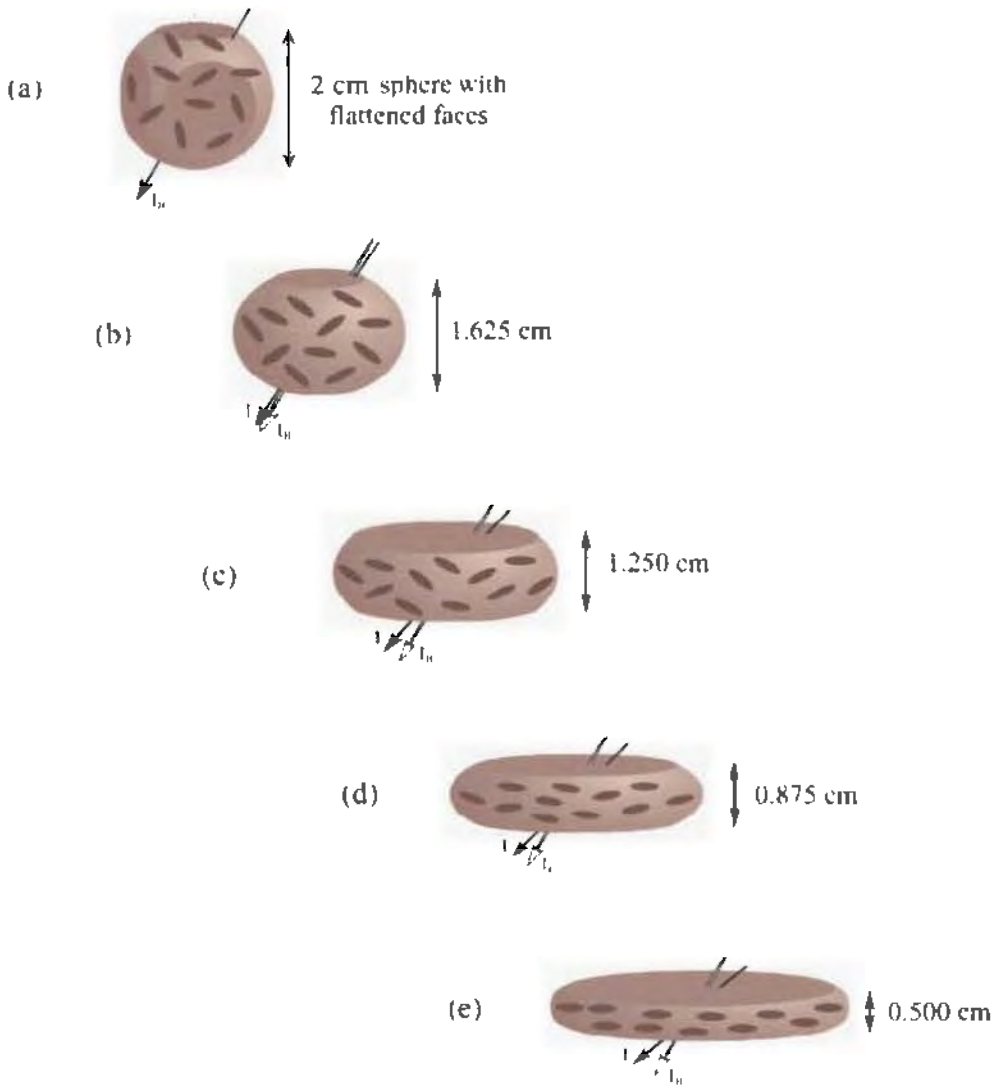


**Figure 3.4** A schematic diagram of the four-step incremental compression experiment. **(a)** The magnetite (dark) grains are randomized by kneading, given flat faces and an inclined ARM, $I_{II}$, imparted to the 2 cm diameter sample. **(b)** The first step of the four-step incremental compression experiment produces a disk of 1.625 cm thickness. The magnetic grains tend to rotate towards the horizontal plane and the inclination of the ARM, $I$, becomes shallower than the original $I_{II}$. The disk is trimmed and measured as in Figure 3.4. **(c)** Without reassembly and kneading, this disk is further compressed to a thickness of 1.250 cm and the grains rotate further and $I$ is further reduced. The disk is again trimmed and measured. **(d)** The disk is compressed to 0.875 cm, trimmed and measured. **(e)** The disk is compressed to a final thickness of 0.5 cm, trimmed and measured. The sample is then reassembled, kneaded to randomize the grains as in (a), etc.

# CHAPTER 4

# USING THE MAGNETIC ANISOTROPY AND INCLINATION SHALLOWING INDUCED BY LABORATORY COMPRESSION TO HELP CORRECT FOR PALEOMAGNETIC INCLINATION SHALLOWING

## 4.1 Using Remanence Anisotropy to Correct for Inclination Shallowing in Core 28

A spherical composite sample of Core 28 (kneaded to make it isotropic and given flat faces) was given an anhysteretic remanence (ARM) of ~60E inclination and compressed as described above in section 3.2. The sample was compressed in a non-magnetic press (Figure 3.1) to a thickness of 1 cm (half compression) producing a disk-shaped sample through plastic deformation. The sample was trimmed to fit into the 2 cm cubic holder and centred vertically in the holder with polystyrene spacers as described in Figure 3.2. Remanence inclination and intensity were then measured. Then $ARM_{min}/ARM_{max}$ was measured as described above (section 2.7). The sample was removed from the holder, the grains were randomized and an ARM of ~60° inclination was given as before. The sample was then compressed to a thickness of 0.5 cm (full compression), stacked as described above (section 3.2) and measured. The one-step compression experiments were repeated six times to 0.5 cm thickness and seven times to 1 cm thickness for Core 28 (Appendix B). The results are plotted

as open circles for the half compression and as closed circles for the full compression in a graph of $\tan I/\tan I_H$ vs $ARM_{min}/ARM_{max}$ (Figure 4.1).

The square of the Pearson product moment coefficient of correlation, $R$, is given ($R$ = .985). This is a measure of the strength of the linear relationship between two variables in a sample, in this case $\tan I/\tan I_H$ and $ARM_{min}/ARM_{max}$ (Mendenhall and Sincich, 1986). It is possible to determine the level of confidence for the linear relationship using the table of critical values given in Appendix E. In this instance, the $R$ calculated for the two variables $\tan I/\tan I_H$ and $ARM_{min}/ARM_{max}$ for this sample size (n=13) ($R$ = 0.985) is greater than the critical value for 95% confidence indicated in the table ($R$ = 0.553). Therefore we can say that we are at least 95% confident of a linear relationship between $\tan I/\tan I_H$ and $ARM_{min}/ARM_{max}$. This method of determining a linear correlation (with greater than 95% confidence) was used throughout this thesis. A definition of $R$ and the table of critical values is given in Appendix E.

There might be a concern that the shape of the compressed and trimmed sample might affect the $ARM_{min}/ARM_{max}$ value. To test whether this concern is justified, the sample was given an ARM of ~60° inclination as above but was compressed in a single compression to 0.5 cm thickness. Then it was cut into four quadrants and stacked as shown in Figure 3.3 eliminating most of the disk's shape anisotropy. This was repeated six times and the results of these six stacking

experiments (squares) are displayed along with the seven trimming experiments (triangles) on the graph of $\tan I/\tan I_H$ vs $ARM_{min}/ARM_{max}$ in Figure 4.2. The two sets of $ARM_{min}/ARM_{max}$ values show no significant difference (other than a greater degree of scatter among the values of the trimming experiments) indicating that any sample shape anisotropy effect is negligible.

The 19 sets of values of $ARM_{min}/ARM_{max}$ and $\tan I/\tan I_H$ from these one-step trimming experiments and stacking experiments were plotted as circles (half-compression) or squares and triangles (full compression) in Figure 4.3 along with the theoretical curves of Jackson et al. (1991). A regression line (and the 95% confidence interval for its slope) was drawn through the 19 experimental data points for Core 28 using the data analysis tool in Microsoft Excel.

As demonstrated by Hodych and Bijaksana (1993), Jackson=s theory predicts that during stepwise compaction a sample should move down a roughly linear curve on $\tan I/\tan I_H$ vs $ARM_{min}/ARM_{max}$ plots. The slope of the line depends upon the average remanence anisotropy ($ARM_\perp/ARM_\parallel$) of the individual magnetite particles in the sample. This assumes elongated magnetite particles with $ARM_\perp$ being the intensity of ARM given perpendicular to the long axis of the magnetite particle and $ARM_\parallel$ being the intensity of ARM given in the same way parallel to the long axis (Figure 1.2). Therefore, it is possible to estimate the particle anisotropy of Core 28 by comparing the slope of the regression line with the roughly linear curves plotted

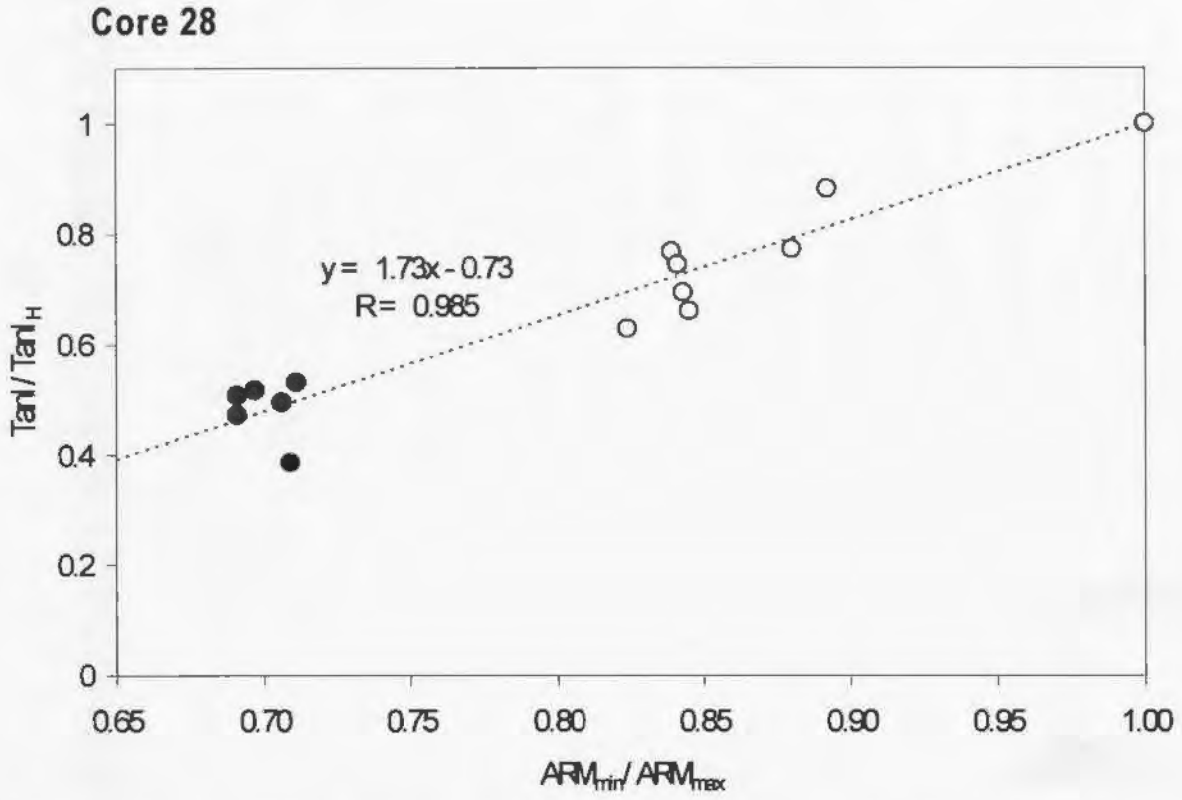


**Figure 4.1** A graph of tan$I$/tan$I_H$ vs $ARM_{min}/ARM_{max}$ obtained from one-step compression experiments to full compression of 0.5 cm thickness (open circles), and half compression of 1.0 cm thickness (closed circles) for a composite sample of Core 28. The equation of a trendline through the data (dashed line) and its associated Pearson product moment coefficient of correlation are given.

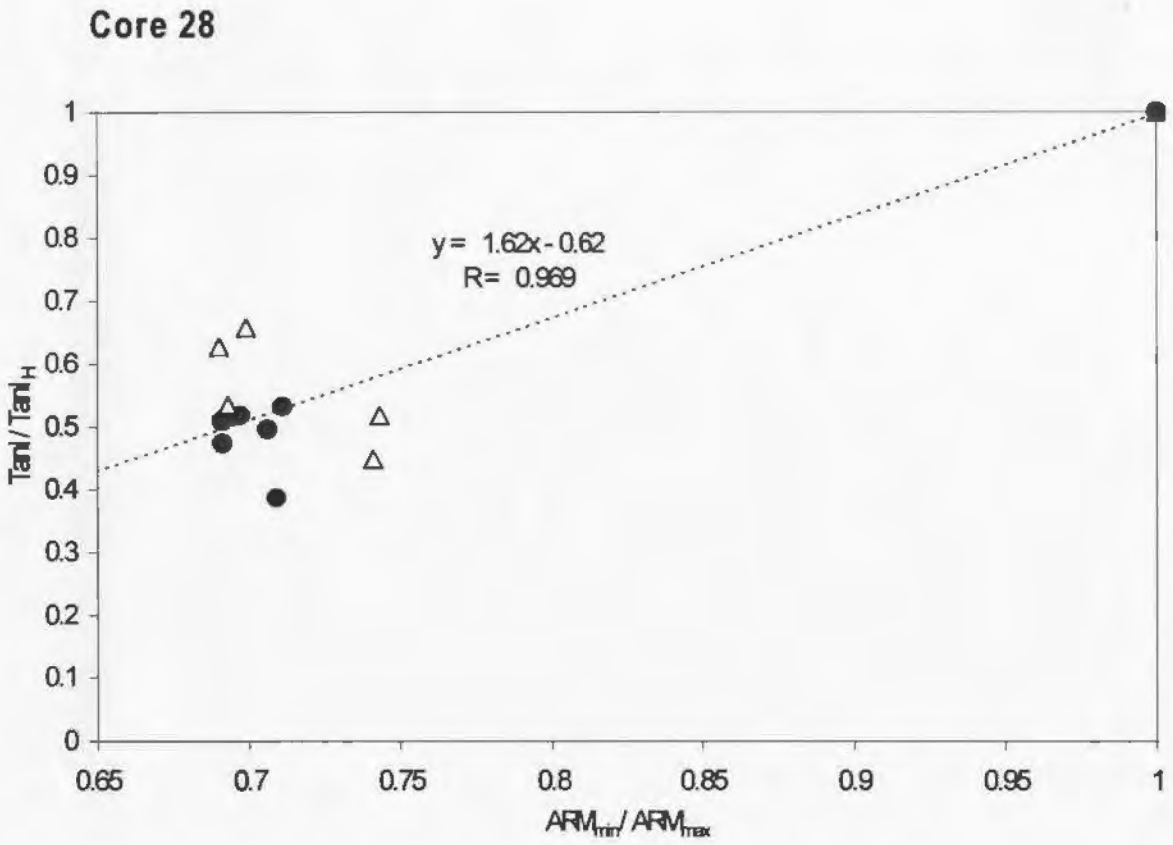


**Figure 4.2** Testing for any shape anisotropy effect by plotting results from one-step full compression experiments to 0.5 cm thickness on a graph of tan$I$/tan$I_H$ vs $ARM_{min}/ARM_{max}$. Data from stacking experiments are closed circles and data from trimming experiments are triangles. There is no significant difference (other than a greater degree of scatter among the values of the trimming experiments) between the two data sets indicating that any sample shape anisotropy effect is negligible. The equation of a trendline through the data (dashed line) and its associated Pearson product moment coefficient of correlation are given.

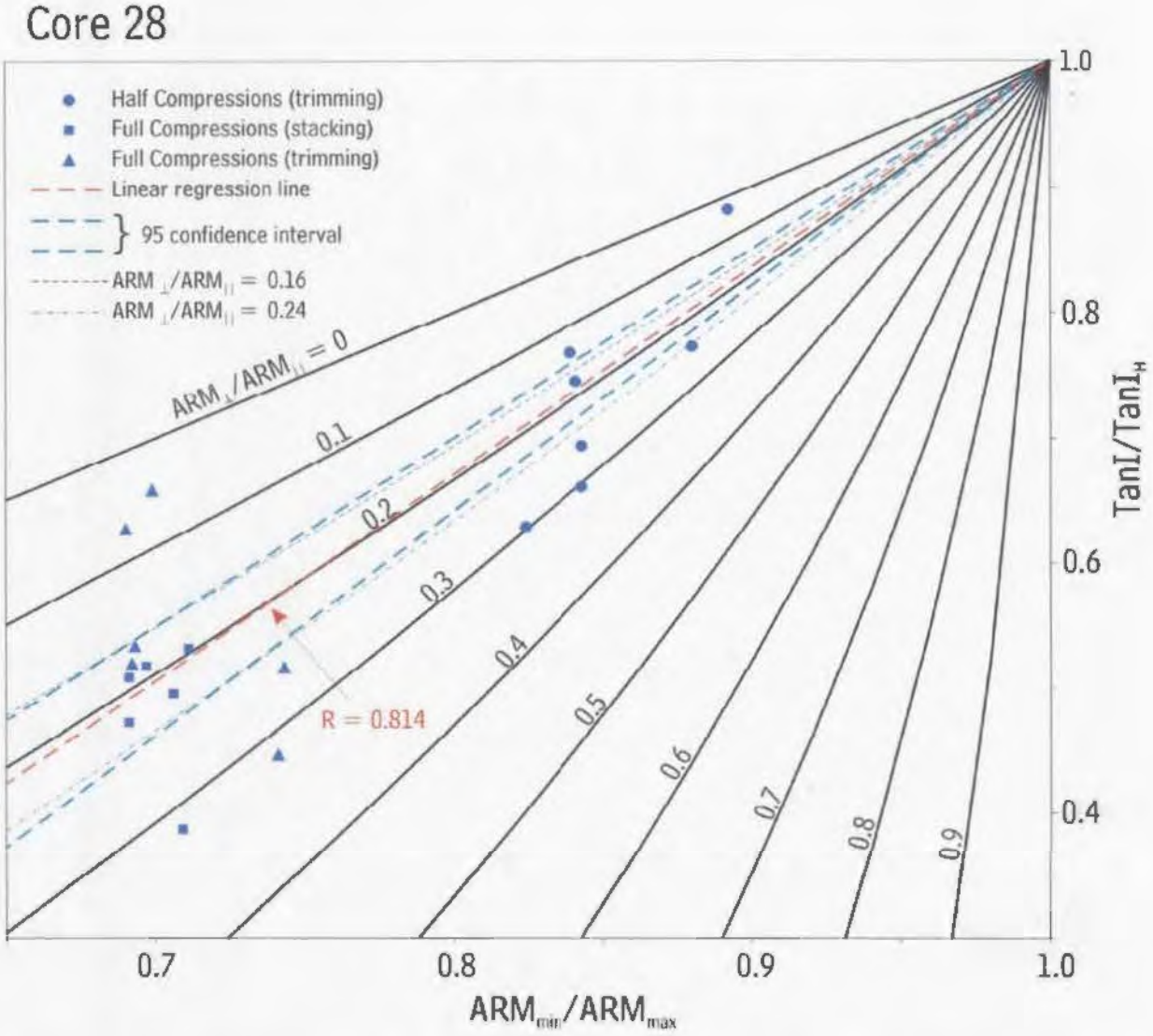


**Figure 4.3** Estimating particle anisotropy ($ARM_{\perp}/ARM_{\parallel}$) by plotting data from seven half compression (circles), six full compression stacking (squares) and six full compression trimming (triangles) experiments using a composite sample from Core 28. The trendline (dashed red line) through the 19 data points estimates $ARM_{\perp}/ARM_{\parallel} \approx 0.200$. The lines representing the 95% confidence interval for the trendline (dashed green lines) estimate upper and lower limits for $ARM_{\perp}/ARM_{\parallel}$ to be 0.24 and 0.16 respectively (dotted lines).

using Jackson's theory (Equation 1.1). The ARM /$ARM_{\parallel}$ of the theoretical curve that best matches the regression line is 0.20 which is considered to be an estimate of the $ARM_{\perp}/ARM_{\parallel}$ of the magnetite particles in the sample (Figure 4.3). The lines representing the 95% confidence interval were similarly matched with theoretical curves to estimate the 95% confidence interval for the particle anisotropy giving $ARM_{\perp}/ARM = 0.20 \pm 0.04$.

The corrected remanence inclination, $I_H$, was estimated for each sample in Core 28 by substituting the estimated average particle anisotropy ($ARM_{\perp}/ARM_{\parallel} = 0.20 \pm 0.04$) into Equation 1.1 along with the observed NRM inclination (I), and the observed remanence anisotropy ($ARM_{min}/ARM_{max}$) for each sample used (listed in Appendix A). The average corrected ChRM inclination is 59.6° with a 95% confidence interval of ±3.7° which includes the 60.6° expected from the geocentric axial dipole model (GAD). The average observed uncorrected inclination was 51.4° ± 3.2° (Table 4.1).

## 4.2 Using Remanence Anisotropy to Correct for Inclination Shallowing in Core 24 and Site 578

Two-step compression experiments were performed using the other cores in this study (Appendix B). For each of these cores the composite sample was prepared, was given an ARM with ~60° inclination ($I_H$), was compressed in a single

**Table 4.1** Summary of results using magnetic anisotropy to correct for compaction-induced paleomagnetic inclination shallowing in clay-rich magnetite-bearing soft sediments.

| Sample | $I_H$ | $I_{obs}$ | Remanence anisotropy compression experiments | | Susceptibility anisotropy compression experiments | | $I_H$ estimate from tan $I$ versus (Hodych et al, 1999) | |
|---|---|---|---|---|---|---|---|---|
| | (GAD) | (average) | $ARM_{\perp}/ARM_{\parallel}$ (a95) | $I_{corrected}$ (a95) | Slope C (a95) | $I_{corrected}$ (a95) | $ARM_{min}/ARM_{max}$ (a95) | $K_{min}/K_{max}$ (a95) |
| Core 28 | 60.6° | 51.4° | 0.200 (+0.040/-0.040) | **59.6°** (+3.7/-3.7) | 2.192 (+0.118/-0.117) | **57.8°** (+3.5/-3.4) | **65.6°** (+4.5/-6.8) | **63.5°** (+4.2/-5.9) |
| Core 24 | 61.1° | 53.8° | 0.345 (+0.035/-0.045) | **63.9°** (+4.5/-5.0) | 2.317 (+0.223/-0.223) | **59.0°** (+4.7/-4.8) | | |
| Site 578 | 53.4° | 48.8° | 0.550 (+0.050/-0.090) | **54.0°** (+4.3/-4.7) | 8.379 (+1.460/-1.460) | **53.1°** (+4.9/-5.0) | | |



$I_H$ (GAD) is the inclination of the Earth=s magnetic field expected from the Geocentric Axial Dipole model at the sample collection site. $I_{obs}$ (average) is the average inclination of the characteristic remanent magnetization in the sediment core. $ARM_{\perp}/ARM_{\parallel}$ (a95) is the particle magnetite anisotropy parameter (and its 95% confidence interval) estimated using change in remanence anisotropy parameter ($ARM_{min}/ARM_{max}$) and in remanence inclination upon compressing a composite sample. The associated $I_{corrected}$ (a95) is the estimate of $I_H$ (and its 95 % confidence interval) corrected for inclination shallowing using $I_{obs}$ and $ARM_{min}/ARM_{max}$ of the natural specimens and the estimate of $ARM_{\perp}/ARM_{\parallel}$ for the composite sample. Slope C (a95) is the slope (and its associated 95% confidence interval) of the regression line through the experimental data points on a graph of $\tan I/\tan I_H$ vs $K_{min}/K_{max}$ observed upon compressing the composite sample. The associated $I_{corrected}$ (a95) is the average estimate of $I_H$ (and its 95% confidence interval) corrected for inclination shallowing using $I_{obs}$ and $K_{min}/K_{max}$ of the natural specimens the estimate of Slope C for the composite sample. The last two columns show the $I_H$ estimate (and its 95% confidence interval) from the correlation between $\tan I_{obs}$ and $ARM_{min}/ARM_{max}$ and from the correlation between $\tan I_{obs}$ and $K_{min}/K_{max}$ for the natural specimens of core 28 by Hodych et al. (1999).

step to 1.0 cm thickness (half compression), trimmed to fit into the holder as described above and remanence inclination $I$ and $ARM_{min}/ARM_{max}$ were measured. This was repeated six times. The sample was then prepared and given an ARM with ~60° inclination ($I_H$), and compressed to 0.5 cm thickness (full compression), cut into quadrants and stacked as described above in section 3.2. Remanence inclination $I$ and $ARM_{min}/ARM_{max}$ were measured. To maintain statistical significance, these half and full compression experiments were repeated six times each for Core 24 and Site 578.

A linear regression line and the 95% confidence interval for its slope was drawn for each core to estimate the average anisotropy parameter $ARM_{\perp}/ARM$ for the magnetite grains in Core 24 as well as Site 578 (Figures 4.4 and 4.5 respectively). The results of these experiments are summarized in Table 4.1. This parameter was used as in Core 28 to correct for inclination shallowing. The 95% confidence interval for estimated inclination using this method contained that predicted by the GAD model for Core 28, Core 24 and Site 578.

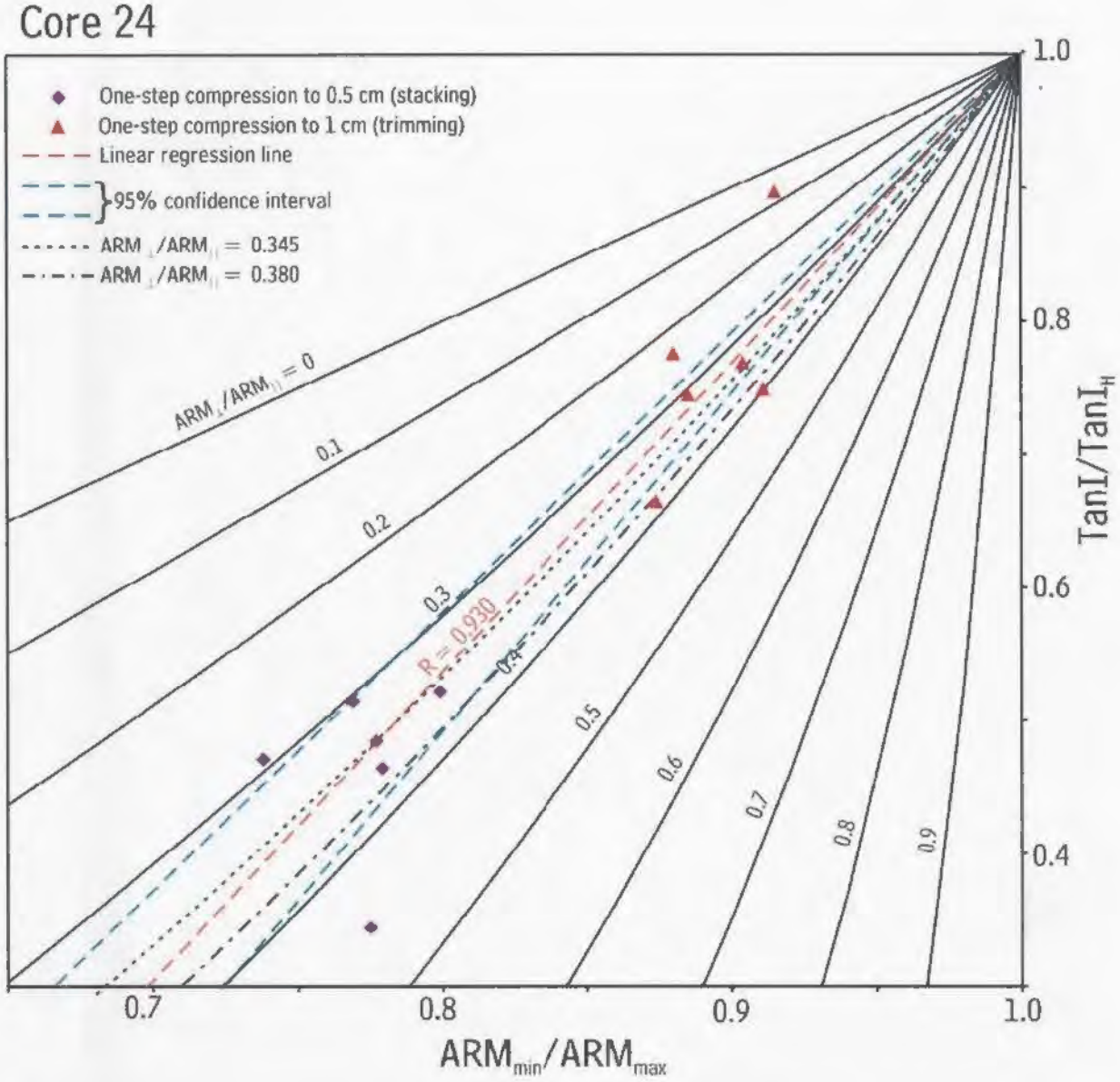


**Figure 4.4** Estimating particle anisotropy ($ARM_{\perp}/ARM_{||}$) by plotting data from six full compression stacking experiments (diamonds) using a composite sample from Core 24. The trendline (dashed red line) through the data estimates $ARM_{\perp}/ARM_{||} \approx 0.345$. The lines representing the 95% confidence interval for the trendline (dashed green lines) estimate upper and lower limits for $ARM_{\perp}/ARM_{||}$ to be 0.400 and 0.280 (dotted line).

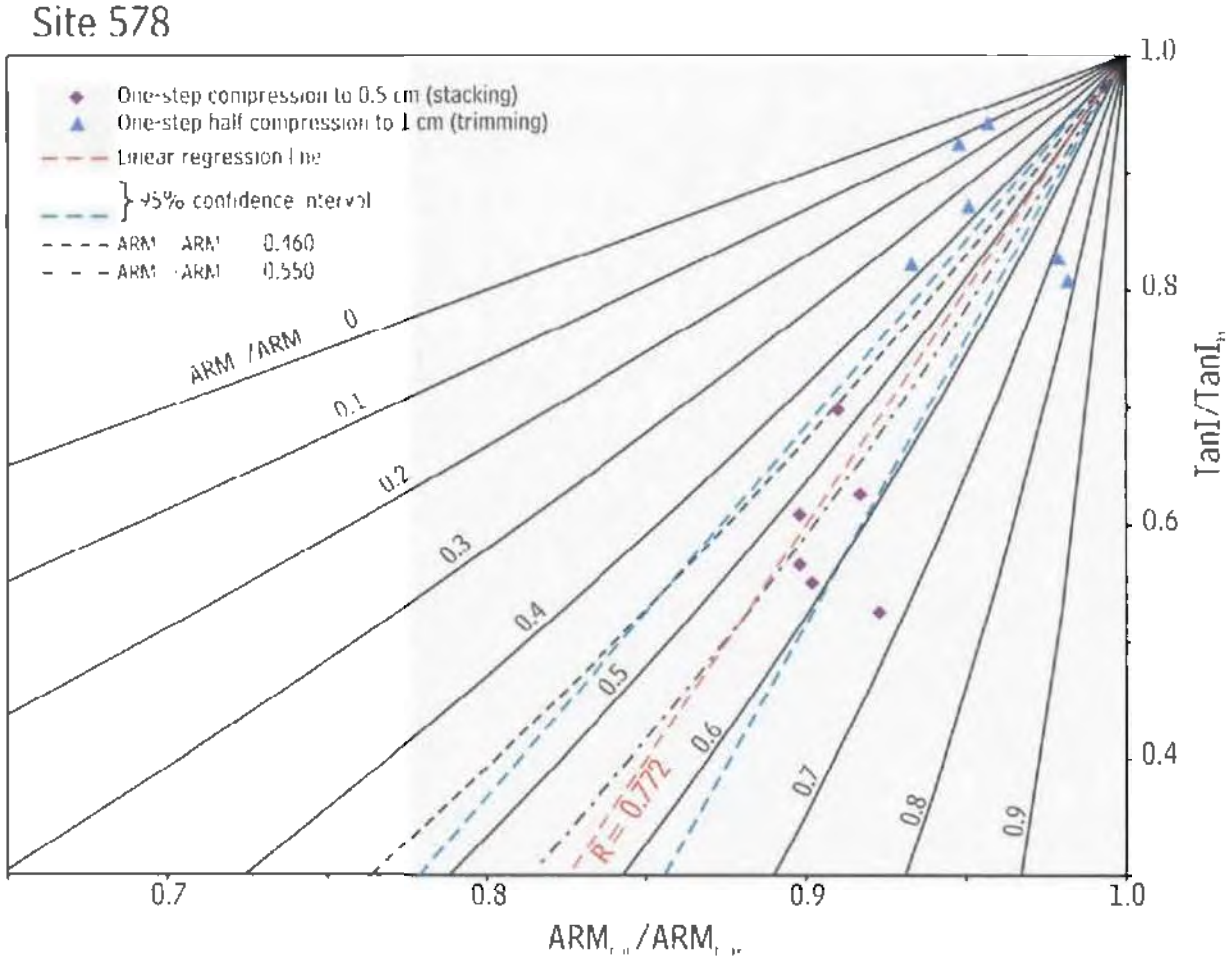


**Figure 4.5** Estimating particle anisotropy ($ARM_{\perp}/ARM$ ) by plotting data from six full compression stacking experiments (diamonds) using a composite sample from Site 578. The trendline (dashed red line) through the data estimates $ARM_{\perp}/ARM \approx 0.625$. The lines representing the 95% confidence interval for the trendline (dashed green lines) estimate upper and lower limits for $ARM_{\perp}/ARM$ to be 0.570 and 0.490 (dotted line).

## 4.3 Using Susceptibility Anisotropy to Correct for Inclination Shallowing in Core 28

Although the compression experiments described above using remanence anisotropy are often effective in correcting for inclination shallowing, they are very time-consuming. This correction method would be much faster if susceptibility anisotropy ($K_{min}/K_{max}$) measurements could be used in place of remanence anisotropy ($ARM_{min}/ARM_{max}$). Not only is $K_{min}/K_{max}$ much faster to measure than $ARM_{min}/ARM_{max}$, but also, the inclined ARM is not destroyed in measuring $K_{min}/K_{max}$, making multi-step compression experiments possible with the same inclined ARM. Although ARM is a better analogue for NRM (natural remanent magnetization) than magnetic susceptibility, Hodych et al. (1999) showed that correcting for inclination shallowing using plots of tan$I$ versus $K_{min}/K_{max}$ instead of plots of tan$I$ versus $ARM_{min}/ARM_{max}$ can succeed (and save time) for magnetite bearing rocks provided the magnetite is not single-domain. All of the samples studied are dominated by pseudo-single-domain magnetite as was demonstrated in $J_R/J_S$ vs $H_{cr}/H_c$ plots for Core 28 (Figure 2.4), Core 24 and Site 578 by Bijaksana (1996). We now test whether compression experiments with susceptibility anisotropy in place of remanence anisotropy can successfully be used to correct for inclination shallowing in these samples.

According to Equation 1.1 from the theory of Jackson et al. (1991), tan$I$/tan$I_{II}$ should be approximately linearly related to $ARM_{min}/ARM_{max}$. Therefore we expect:

$$\frac{\tan I}{\tan I_{II}} \approx B\frac{ARM_{min}}{ARM_{max}} + 1 - B \qquad (4.1)$$

where B is the slope of a regression line on a graph of tan$I$/tan$I_{II}$ vs $ARM_{min}/ARM_{max}$ (full derivation in Appendix D). We further expect (Hodych et al., 1999) that the susceptibility anisotropy ($K_{min}/K_{max}$) should be approximately linearly related to tanI/tan$I_{II}$ provided that the magnetite particles are not single-domain. This yields:

$$\frac{\tan I}{\tan I_{II}} \approx C\frac{K_{min}}{K_{max}} + 1 - C \qquad (4.2)$$

where C is the slope of a regression line through the experimental data on a graph of tan$I$/tan$I_{II}$ vs $K_{min}/K_{max}$. This relationship should be valid for the specimens studied since the magnetite in the specimens was determined to be pseudo-single-domain (Bijaksana, 1996).

A composite sample was prepared for Core 28 as described in the previous section. That is, it was kneaded to make it isotropic, given an ARM of inclination $I_{II}$ ~60E and then compressed. The sample was initially compressed to a thickness of 1.625 cm and then trimmed as described in section 3.3 to fit in the 2 cm cubic holder, and vertically centred with spaeers (Figure 3.2). Susceptibility anisotropy parameter

$K_{min}/K_{max}$ and remanence inclination $I$ were measured. The sample was removed from the holder and further compressed to a thickness of 1.250 cm, trimmed and $K_{min}/K_{max}$ and $I$ were measured again. This was then repeated compressing to a thickness of 0.875 cm and finally to 0.500 cm. Once this four-step incremental compression experiment was repeated 6 times, the 30 experimental values (Appendix C) were plotted on a graph of $\tan I/\tan I_{II}$ vs $K_{min}/K_{max}$ (Figure 4.6).

The graph of $\tan I/\tan I_{II}$ vs $K_{min}/K_{max}$ (Figure 4.6) for Core 28 confirms that the data points do move roughly down along a straight line during stepwise compression as was predicted by Equation 4.2. Linear regression analysis using the Data Analysis add-in tool in Microsoft Excel shows that the correlation is significant at the 95% confidence interval ($R = 0.967$, exceeding 0.361). The correlation line yielded a slope C of 2.19 with a 95% confidence interval of ±0.1. This value of C and the observed values of $\tan I$ and $K_{min}/K_{max}$ from each of the original core specimens (Appendix A) were used in Equation 4.2 to estimate $I_{II}$ from each specimen. The average $I_{II} = 57.8°$ (+3.5/3.4) which includes the 60.6° expected from the GAD model. (The average uncorrected inclination was 51.4°±3.2°).

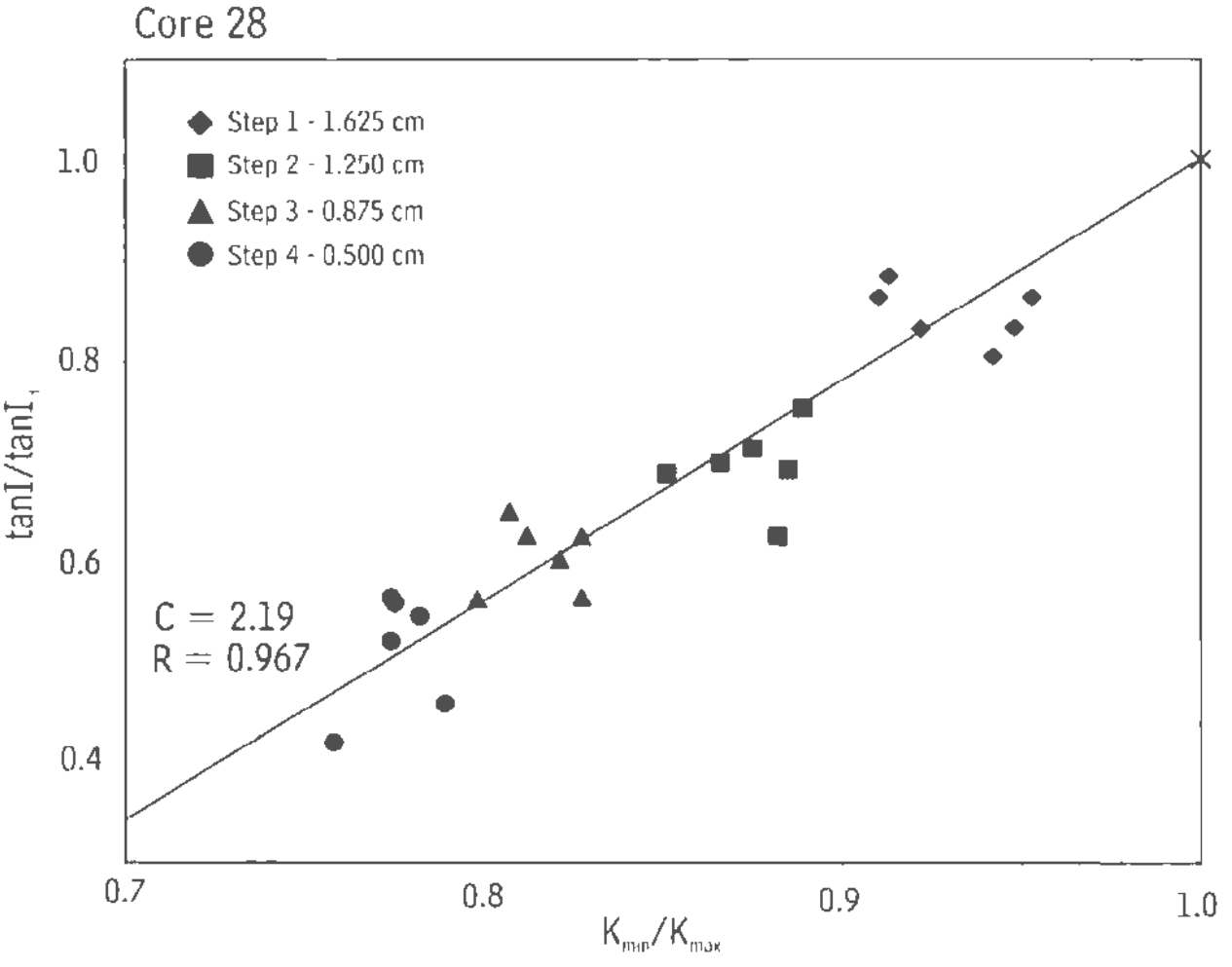


**Figure 4.6** Data from six four-step incremental compression experiments using a composite sample from Core 28 are plotted on a graph of $\tan I/\tan I_i$ vs $K_{min}/K_{max}$. The starting state of each experiment with randomized grains (no anisotropy) and no inclination shallowing is given by a cross. The six values from each step of the cumulative compression experiments to thicknesses of 1.625 cm, 1.250 cm, 0.875 cm and 0.500 cm are plotted as diamonds, squares, triangles and circles respectively. A trendline through the data has slope C = 2.19 with a 95% confidence interval of ±0.12 (R = 0.967, exceeding 0.361).

## 4.4 Using Susceptibility Anisotropy to Correct for Inclination Shallowing in Core 24 and Site 578

For both Core 24 and Site 578 two-step compression experiments to thicknesses of 1.0 and 0.5 cm were performed (Appendix B). The one-step compression experiment to 1.0 cm thickness using the trimming technique was repeated 6 times for core 24 and Site 578 while the compression technique to 0.5 cm thickness using stacking was repeated 6 times for the Core 24 and 4 times for Site 578 composite samples. Using these two-step compression experiments successfully corrected for inclination shallowing for both cores, although each has a slightly larger associated 95% error than for Core 28 using four-step incremental compression experiments. Linear regression analysis using the Data Analysis tool in Microsoft Excel yielded a slope C of 2.317 for Core 24 with a 95% confidence interval of +0.223/-0.224 (Figure 4.7). This value of C and the observed values of tan$I$ and $K_{min}/K_{max}$ from the original core were used in Equation 1.1 to estimate the average tan$I_H$ = 59.0° (+4.7/4.85) which includes the 61.1° expected from the GAD model. (The average uncorrected inclination was 53.8°±4.5°).

For Site 578, linear regression using the Data Analysis tool in Microsoft Excel yielded a slope C of 8.38 with a 95% confidence interval of +1.460/-1.460 (Figure 4.8). This value of C and the observed values of tan$I$ and $K_{min}/K_{max}$ from the original core were used in Equation 1.1 to estimate the average tan$I_H$ - 53.1° (+4.9/5.0)

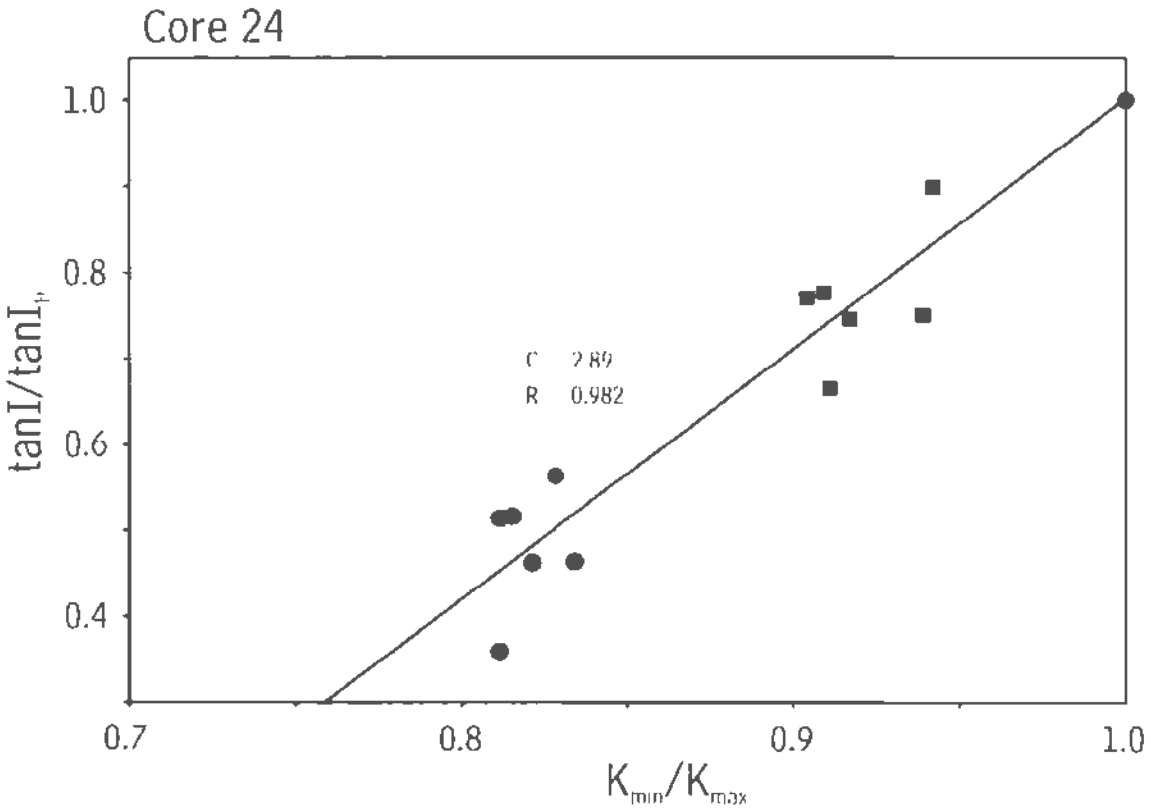


**Figure 4.7** Data from six two-step compression experiments using a composite sample from Core 24 are plotted on a graph of tan$I$/tan$I_{II}$ vs $K_{min}/K_{max}$. A trendline through the data has slope C = 2.89 with a 95% confidence interval of ±0.22 (R = 0.982, exceeding 0.404).

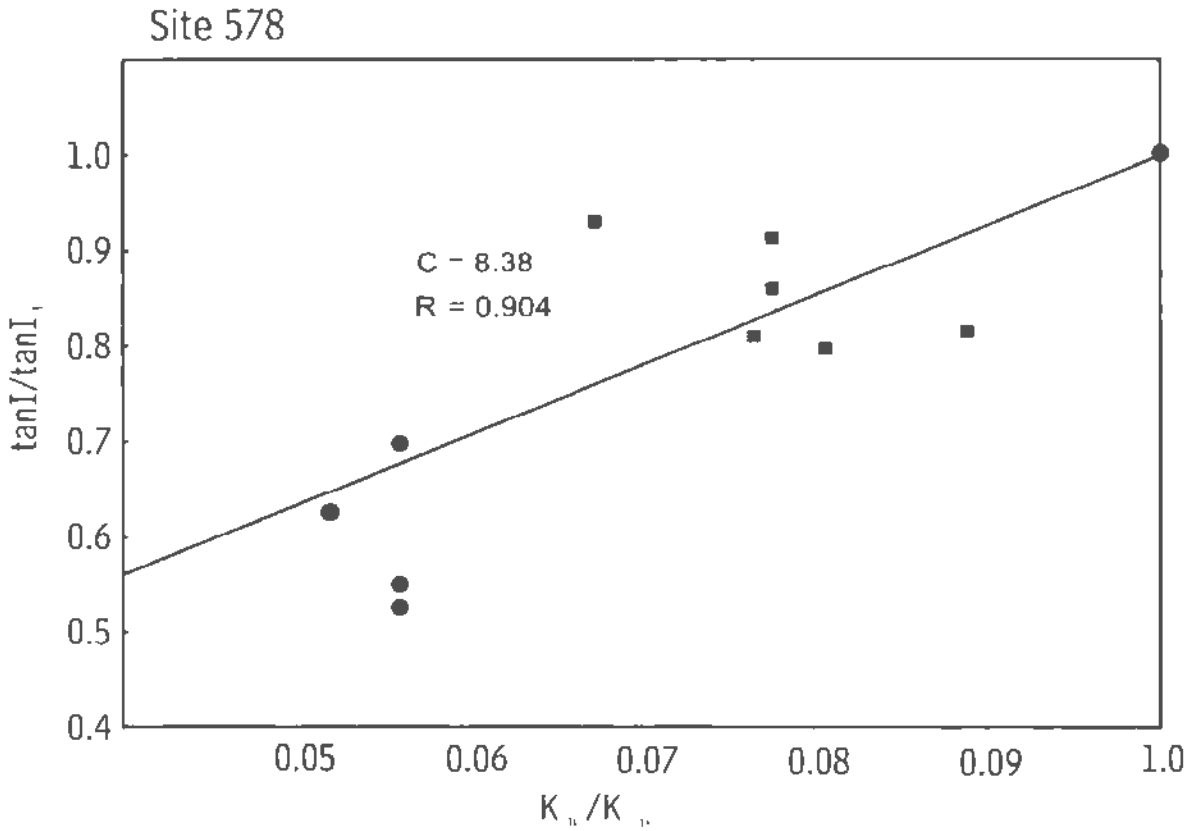


**Figure 4.8** Data from two-step compression experiments using a composite sample from Site 578 are plotted on a graph of tan$I$/tan$I_{II}$ vs $K_{min}/K_{max}$. A trendline through the data has slope C = 8.38 with a 95% confidence interval of ±1.46 (R = 0.904, exceeding 0.444).

which includes 53.4° as expected from the GAD model. (The average uncorrected inclination was 48.8°±3.7°.) The results for all these experiments are summarized in Table 4.1.

# CHAPTER 5

# REMANENCE INTENSITY DECREASE INDUCED IN THE LABORATORY COMPRESSION EXPERIMENTS: IMPLICATIONS FOR PALEOINTENSITY STUDIES USING PISTON CORES

## 5.1 Compaction-Induced Decrease in Remanence Intensity

The intensity of the Earth's magnetic field changes constantly and how it has changed in the past is of much interest. Lava flows and baked clays can yield accurate paleointensity estimates for specific times in the past but usually do not give a continuous record. The detrital remanence of magnetite-bearing sediments has the potential to provide a more continuous record of paleointensity. One of the problems sediments present is the variability in their remanence intensity that occurs through variation in magnetite content in a sedimentary sequence. Various methods of correcting for this variation have been proposed involving normalizing to ARM, SIRM or susceptibility of the sediment samples (Merrill et al., 1996).

The effect of compaction on remanence intensity in sediments and their paleointensity record can also be large but has received little attention. In a review of relative paleointensity in sediments, Tauxe (1993) examined the data of Anson and Kodama (1987) who studied laboratory compaction of sediments. Anson and

Kodama (1987) found that remanence intensity decreased during compaction and suggested that this was due to increased particle interaction, whereas Tauxe (1993) suggests that "it is more likely due to random rotation about a horizontal axis, leading to reduced inclination and reduced intensity." Because compaction-induced magnetic anisotropy has been successfully used to correct for inclination shallowing, we reasoned that magnetic anisotropy might also help correct for compaction-induced intensity decrease. This led us to look for an empirical relation between remanence intensity and magnetic anisotropy in our compression experiments, and resulted in what we believe to be the first attempt to use magnetic anisotropy to correct for compaction-induced decrease in remanence intensity.

## 5.2 Using Magnetic Anisotropy to Estimate Compaction-Induced Decrease in Remanence Intensity in Core 28

Remanence intensity measurements were made during all the compression experiments described above and are tabulated in Appendices B and C as the ratio of remanence intensity after compression (J) to remanence intensity before compression ($J_o$). Note that these remanence intensities are per unit volume of sample and have been corrected for the reduction in sample volume that occurs in those compression experiments in which the sample is trimmed to fit into the sample holder (Figure 3.2).

Figure 5.1 plots $J/J_o$ versus $ARM_{min}/ARM_{max}$ for five one-step "half" compression experiments to 1 cm thickness (open circles) and six one-step "full"

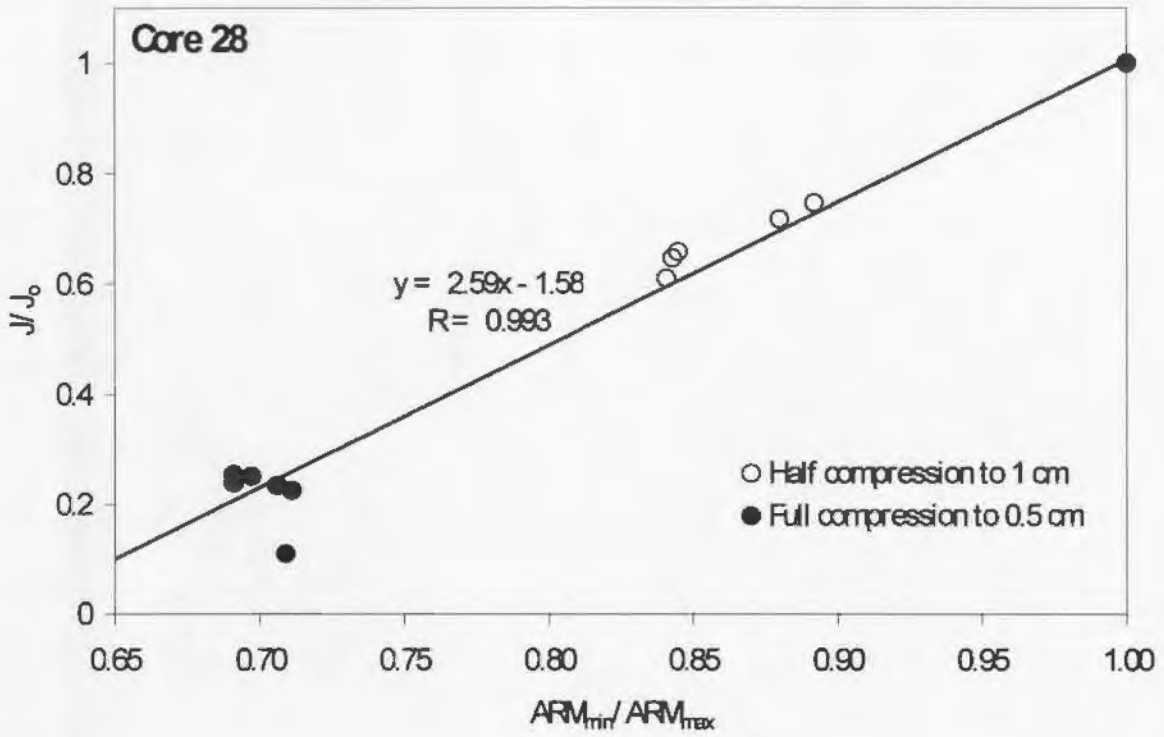


**Figure 5.1** A plot of normalized remanence intensity, $J/J_o$, versus remanence anisotropy parameter, $ARM_{min}/ARM_{max}$, from 5 half compression experiments (open circles) and 6 full compression experiments (closed circles). The data demonstrate a linear correlation that is significant with greater than 95% confidence (R = 0.993 exceeds 0.423). The equation of the regression line is $J/J_o = 2.59(ARM_{min}/ARM_{max}) - 1.58$.

compression experiments to 0.5 cm thickness (closed circles) for the Core 28 composite sample. A linear correlation is found between normalized remanence intensity, $J/J_o$, and the remanence anisotropy parameter, $ARM_{min}/ARM_{max}$, and the correlation is significant with better than 95% confidence ($R = 0.993$ exceeds 0.423). The equation of the correlation line is $J/J_o = 3.36(ARM_{min}/ARM_{max}) - 2.33$. Assuming that this same linear correlation held true during the original burial compaction of the Core 28 sediment, it is possible to estimate $J_o$, the original remanence intensity prior to burial compaction. For each Core 28 specimen, the observed NRM intensity, J, and $ARM_{min}/ARM_{max}$ (Appendix A) were substituted in the equation of the correlation line (Figure 5.1) to estimate the pre-compaction remanence intensity, $J_o$. These resulting $J_o$ values were then divided by the anhysteretic susceptibility, $K_{arm}$ of each specimen (Appendix A) to give relative paleointensity corrected for variation in the amount of magnetite in specimen to specimen. The resulting relative paleointensity is plotted versus depth in Figure 5.2 (dashed line). The uncorrected relative paleointensity (NRM intensity J divided by $K_{arm}$) for each specimen is also plotted versus depth in Figure 5.2 (solid line).

An empirical correlation between normalized remanence intensity $J/J_o$ and the susceptibility anisotropy parameter $K_{min}/K_{max}$ was also observed in Core 28. (The remanence intensity at each incremental step was corrected for volume change due to trimming the sample by dividing it by the average magnetic susceptibility, $K_{mean}$ as described above.) The values of $J/J_o$ and $K_{min}/K_{max}$ for 6 four-step incremental

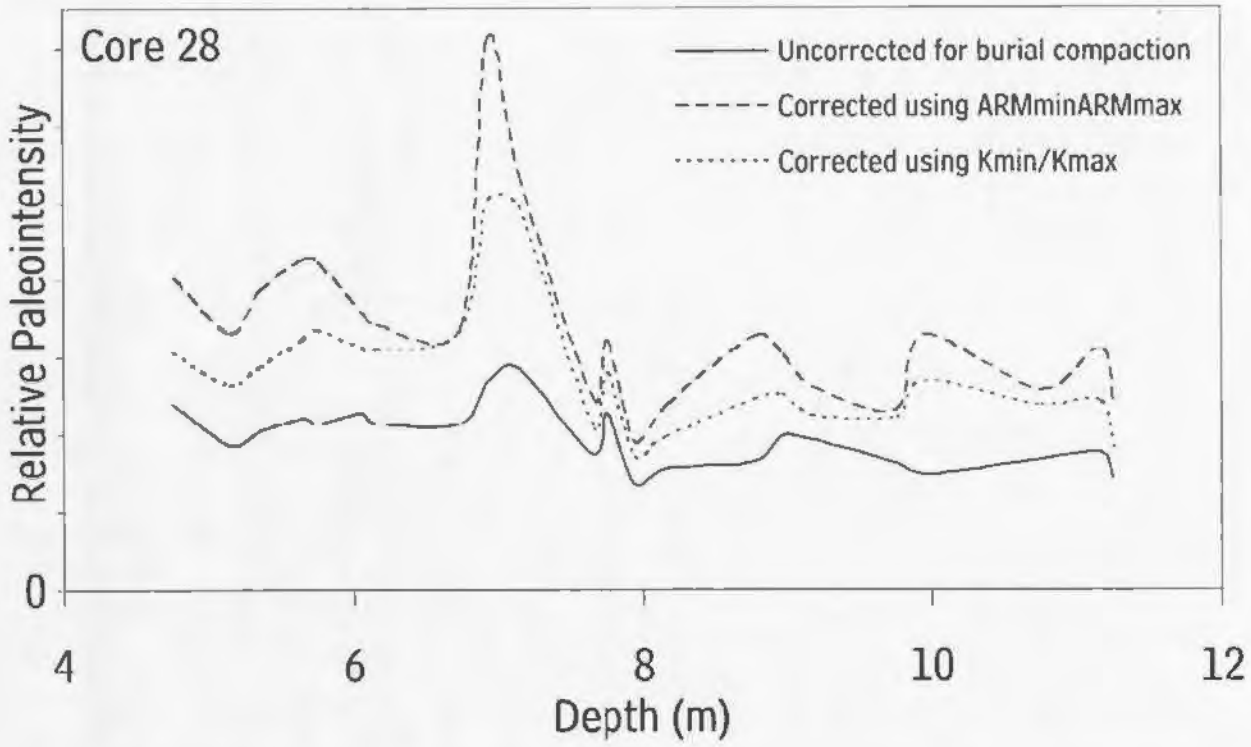


**Figure 5.2** Relative paleointensity plots versus depth in Core 28. The solid line is the uncorrected relative paleointensity of the Earth's field estimated from NRM intensity (J in Appendix A) divided by the anhysteretic susceptibility, ($K_{arm}$). The dashed line is the relative paleointensity corrected for burial compaction using the correlation between $J/J_o$ and $ARM_{min}/ARM_{max}$ in the compression experiments. The dotted line is the relative paleointensity corrected for burial compaction using the correlation between $J/J_o$ and $K_{min}/K_{max}$ in the compression experiments.

compression experiments are plotted in Figure 5.3. The linear correlation between $J/J_o$ and $K_{min}/K_{max}$ is significant with greater than 95% confidence ($R = 0.976$, exceeding .361). The equation of the correlation line is $J/J_o = 2.87(K_{min}/K_{max}) - 1.87$. Assuming that this same linear correlation held true during the original burial compaction of the sediment, the NRM intensity, J, and $K_{min}/K_{max}$ (Appendix A) were used in the equation of the correlation line (Figure 5.3) to estimate the pre-compaction remanence intensity, $J_o$, for each specimen from Core 28. For each specimen, the resulting $J_o$ value was divided by the anhysteretic susceptibility, $K_{arm}$, of the specimen to correct for variation in magnetite content from specimen to specimen. The resulting relative paleointensity estimate ($J_o/ K_{arm}$) is plotted versus depth in Core 28 in Figure 5.2 (dotted line).

## 5.3 Using Magnetic Anisotropy to Estimate Compaction-Induced Decrease in Remanence Intensity in Core 24 and Site 578

The data from the two-step compression experiments using the composite sample from Core 24 were also plotted on graphs of $J/J_o$ vs $ARM_{min}/ARM_{max}$ and $J/J_o$ vs $K_{min}/K_{max}$ (Figure 5.4 a and b). There may not be enough variation in the data points to demonstrate that there is a linear correlation in either case. However, trendlines have been drawn on the assumption that near-linear correlations probably do exist because of their presence in the composite sample from Core 28. For Core 24, the original precompaction remanence intensity, $J_o$, was estimated for each

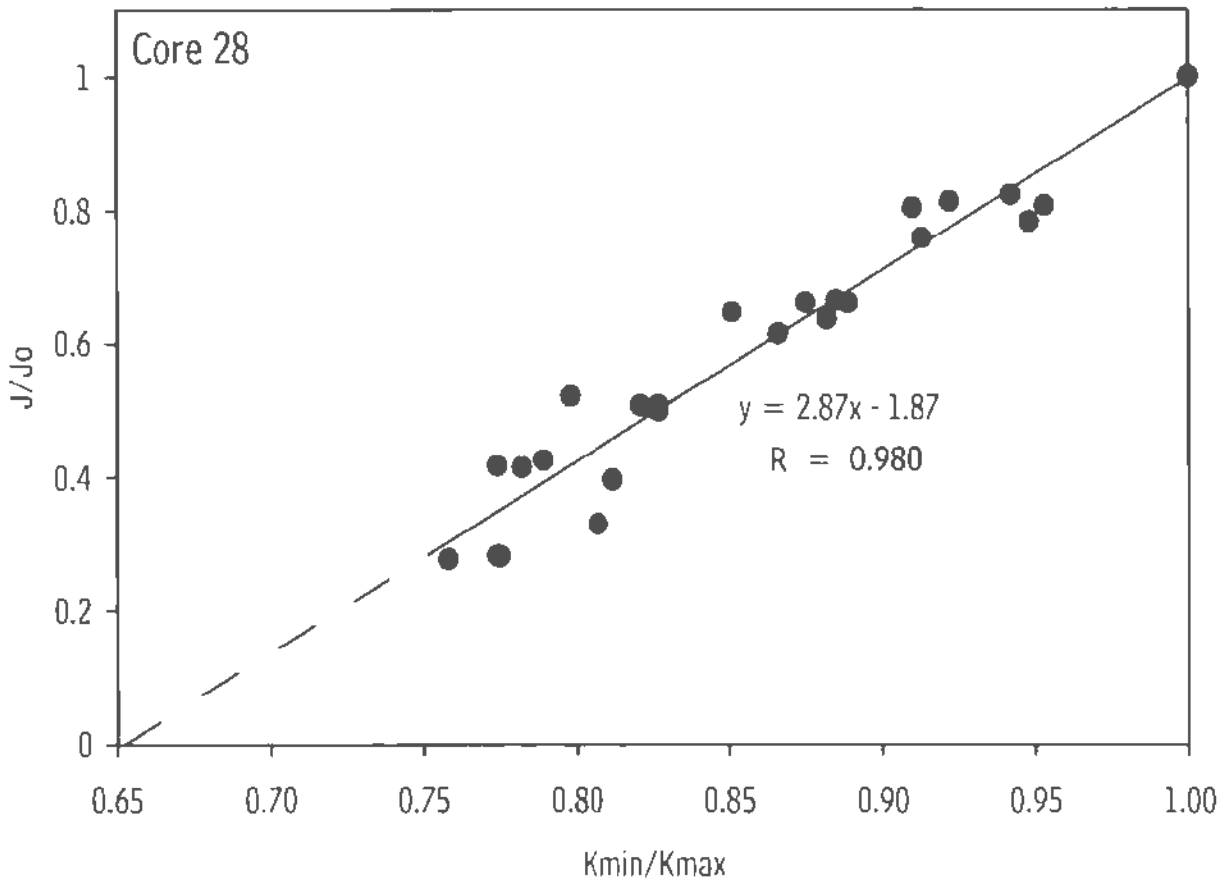


**Figure 5.3** A plot of normalized remanence intensity, $J/J_o$, versus susceptibility anisotropy parameter, $K_{min}/K_{max}$, from six four-step incremental compression experiments on the Core 28 composite sample. The data show a linear correlation that is significant with 95% confidence (R = 0.980 exceeding .423). The equation of the regression line is $J/J_o = 2.87(ARM_{min}/ARM_{max}) - 1.87$.

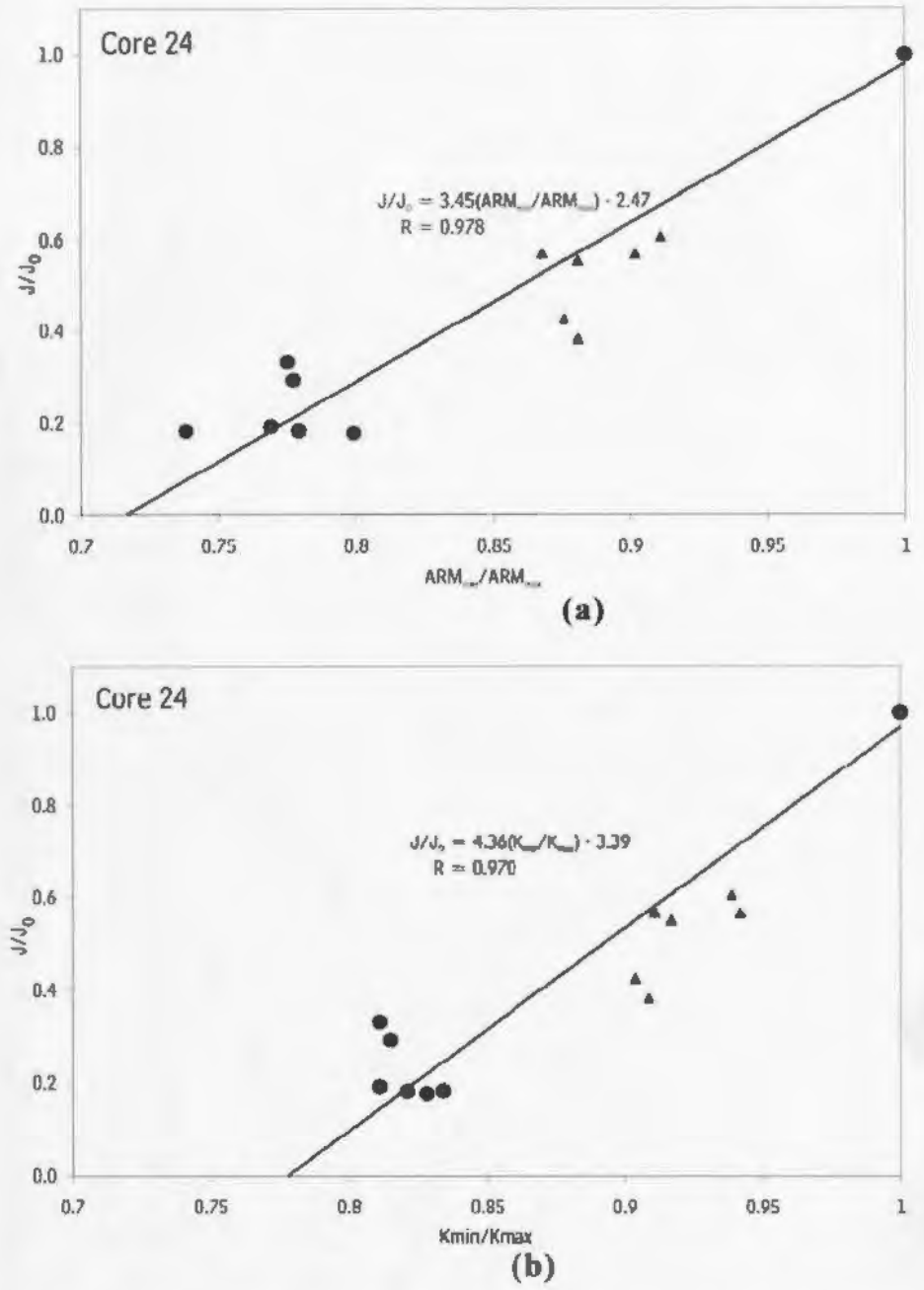


**Figure 5.4 (a)** A plot of normalized remanence intensity, $J/J_o$, versus $ARM_{min}/ARM_{max}$ from six two-step full compression experiments. The equation of a trendline through the data is given. **(b)** A plot of normalized remanence intensity, $J/J_o$, versus $K_{min}/K_{max}$ from six two-step full compression experiments. The equation of a trendline through the data is given.

natural specimen by substituting its NRM intensity (J) and its $ARM_{min}/ARM_{max}$ values into the equation of the trendline (Figure 5.4a) given by $J/J_o = 3.45(ARM_{min}/ARM_{max}) - 2.47$. Dividing this $J_o$ by $K_{arm}$ for each specimen yields a corrected relative paleointensity versus depth plot (the dashed line of Figure 5.5). The trendline $J/J_o = 4.36(K_{min}/K_{max}) - 3.39$ was similarly used with J and $K_{min}/K_{max}$ values for each natural specimen to generate the other corrected relative paleointensity versus depth plot of Figure 5.5 (dotted line).

The NRM intensity prior to compaction was estimated in an analogous manner for each specimen of Site 578 using $J/J_o$ versus $ARM_{min}/ARM_{max}$ or $K_{min}/K_{max}$ plots (Figure 5.6) and the relative paleointensity plots versus depth are given in Figure 5.7.

## 5.4 Discussion

The method suggested above for estimating compaction-induced decrease in remanence intensity using remanence anisotropy should be more reliable than the method using susceptibility anisotropy. (Indeed, using susceptibility anisotropy should only be possible if the magnetite is not single-domain.) Both methods suggest that compaction-induced decrease in remanence intensity can have a serious effect upon relative paleointensity estimates in sediments and sedimentary rocks. However, neither method is very reliable since the linear relation observed during compression between remanence intensity and magnetic anisotropy parameter $ARM_{min}/ARM_{max}$ or $K_{min}/K_{max}$ is purely empirical and it is not certain that the same relation holds during

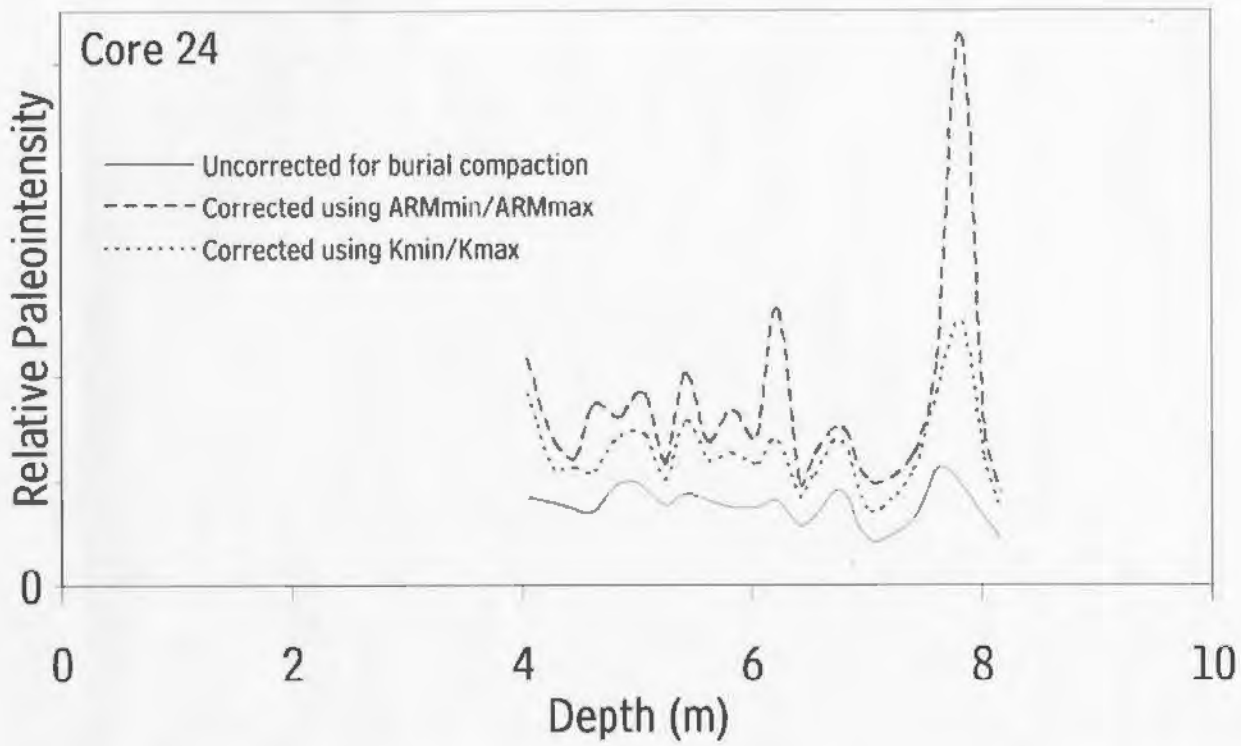


**Figure 5.5** Relative paleointensity plots versus depth in Core 24. The solid line is the relative paleointensity of the Earth's magnetic field estimated from the NRM (J in Appendix A) divided by the anhysteretic susceptibility, ($K_{arm}$). The dashed line is this relative paleointensity corrected for burial compaction assuming a linear relation between $J/J_o$ and $ARM_{min}/ARM_{max}$ in the compression experiments. The dotted line is the relative paleointensity corrected for burial compaction assuming a linear relation between $J/J_o$ and $K_{min}/K_{max}$ in the compression experiments.

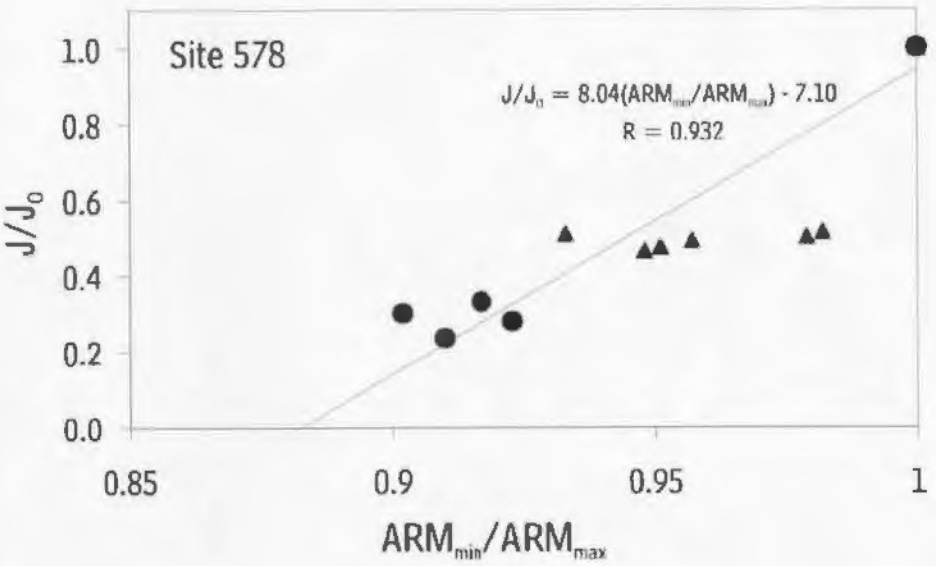


**(a)**

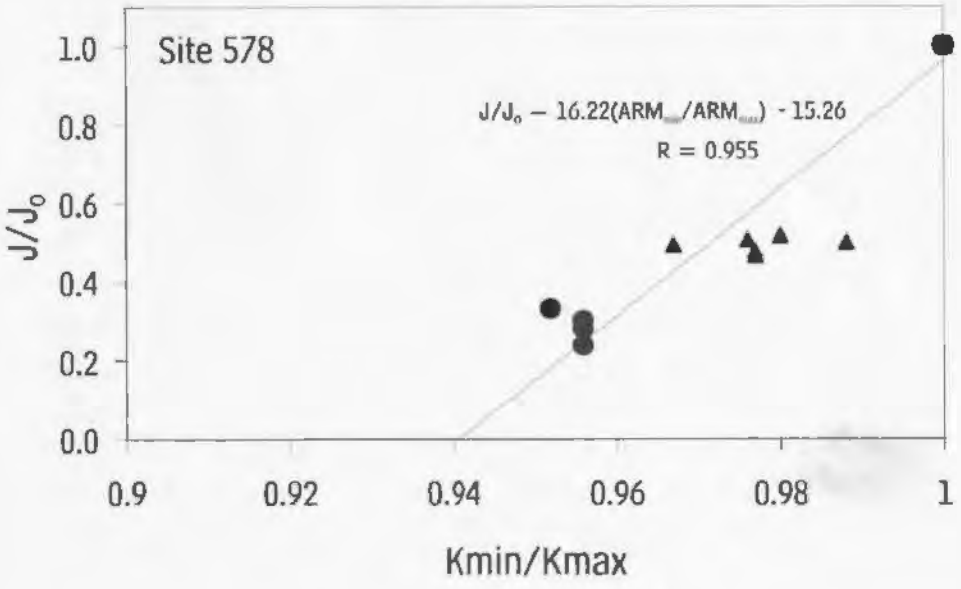


**(b)**

**Figure 5.6 (a)** A plot of normalized remanence intensity, $J/J_o$, versus $ARM_{min}/ARM_{max}$ from four two-step compression experiments. The equation of a trendline through the data is given. **(b)** A plot of normalized remanence intensity, $J/J_o$, versus $K_{min}/K_{max}$ from six two-step compression experiments. The equation of a trendline through the data is given.

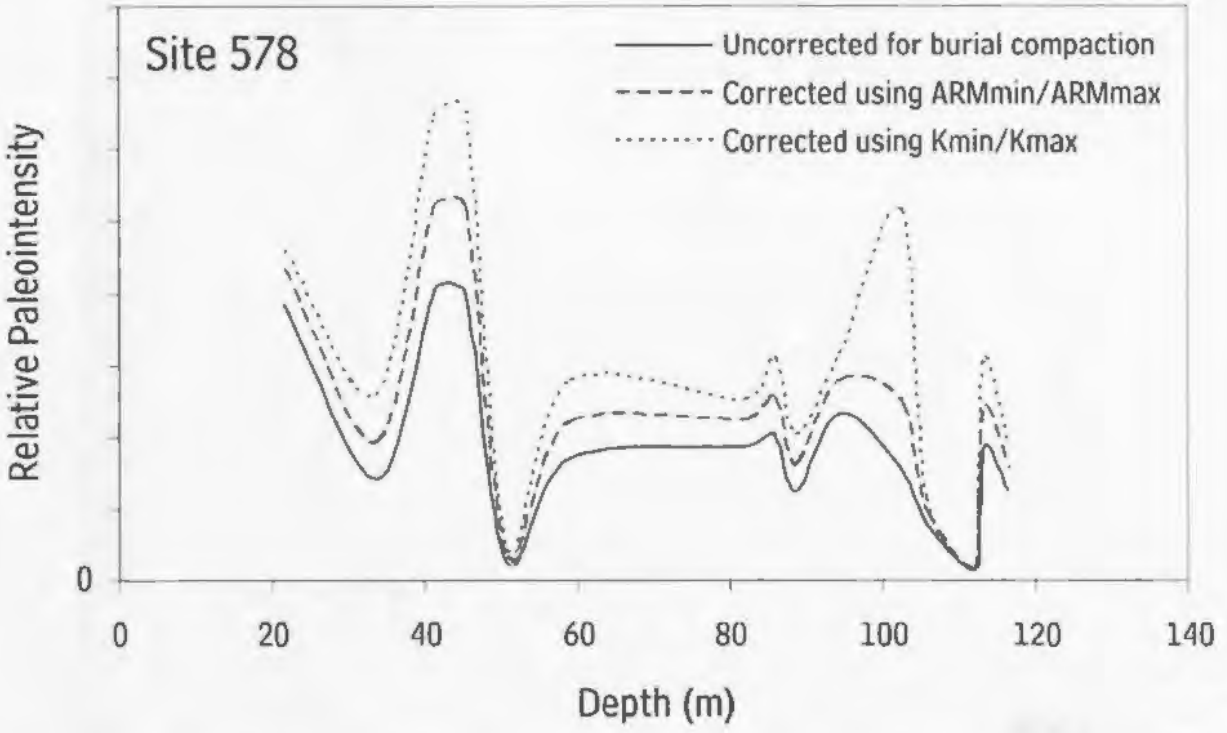


**Figure 5.7** Relative paleointensity plots versus depth at Site 578. The solid line is the uncorrected relative paleointensity of the Earth's magnetic field estimated from the NRM (J in Appendix A) divided by the anhysteretic susceptibility, ($K_{arm}$). The dashed line is the relative paleointensity corrected for burial compaction assuming a linear relation between $J/J_o$ and $ARM_{min}/ARM_{max}$ in the compression experiments. The dotted line is the relative paleointensity corrected for burial compaction assuming a linear between $J/J_o$ and $K_{min}/K_{max}$ in the compression experiments.

burial compaction. Also, the relation must become non-linear at high compression or compaction since $J/J_o$ cannot become smaller than zero. It is possible that the Core 24 or Site 578 data points are already in the non-linear range as may be indicated by how the half-compaction and full-compaction data plot on opposite sides of the regression line. Finally, the age of the sediments and how it varies with depth is poorly known for our cores. Hence we cannot compare our estimates with reliable paleointensity determinations to test their reliability. Nevertheless, the results show that this approach is promising and worth further study.

# CHAPTER 6

# CONCLUSIONS

## 6.1 Correcting for Inclination Shallowing Using Remanence Anisotropy and Uniaxial Compression Experiments

For fine-grained sediment with elongated magnetite grains, burial compaction is expected to rotate the long axes of the magnetite grains towards the horizontal plane causing a shallowing of remanence inclination, $I$, from the inclination of the Earth's magnetic field, $I_H$, in which the sediment was deposited. This compaction also makes it easier to give the sediment an anhysteretic remanence parallel rather than perpendicular to bedding. The theory of Jackson et al. (Equation 1.1) predicts that one can correct for paleomagnetic inclination shallowing in a sediment sample if one measures the remanence anisotropy parameter $ARM_{min}/ARM_{max}$ of the sediment sample (which is the ratio of intensities of anhysteretic remanent magnetization, ARM, given identically perpendicular and parallel to bedding) and the average remanence anisotropy parameter $ARM_{\perp}/ARM$ of the magnetite grains in the sediment (which is the ratio of ARM intensities given identically parallel and perpendicular to the long axes of the magnetite grains). The latter is often difficult to measure. This thesis demonstrates the feasibility of a method (Hodych and Bijaksana, 2002) of estimating $ARM_{\perp}/ARM$ of a suite of magnetite-bearing clay-rich soft sediments that

involves giving a composite sample of the sediment an inclined ARM and vertically compressing it by varying amounts. The plastic deformation of the sediment rotates the ARM towards the horizontal plane and makes it easier to give an ARM parallel to the horizontal plane. For a composite sample from piston Core 28, these compression experiments yielded a linear correlation between $\tan I/\tan I_H$ and $ARM_{min}/ARM_{max}$ (Figure 4.1) as expected from Equation 1.1 (Figure 1.2). The slope of the correlation line yielded an estimate of the average remanence anisotropy parameter $ARM_\perp/ARM_\parallel = 0.200$ (with 95% confidence interval +0.040/-0.040) for the magnetite particles in the Core 28 sediment. Using this estimate of $ARM_\perp/ARM_\parallel$ along with the observed characteristic remanence inclination, $I$, and the remanence anisotropy parameter $ARM_{min}/ARM_{max}$ from the natural specimens of Core 28 provided an estimate of $I_H$ that did successfully correct for compaction-induced inclination shallowing. The $I_H$ estimate was 59.6° with a 95% confidence interval of +3.6/-3.7 which contains the 60.6° field inclination expected from the geocentric axial dipole (GAD) model (whereas the average characteristic remanence inclination was 51.4°).

A simplification of this procedure using two compression steps was performed using a composite sample from piston Core 24 and a composite sample from the Site 578 piston core. For the composite sample from Core 24, the trendline line through the data provided an estimate of $ARM_\perp/ARM_\parallel = 0.345$ with 95% confidence interval +0.035/-0.045. This gives an estimate of $I_H = 63.9°$ with 95% confidence interval

+4.5/-5.0 which contains the 61.1° field inclination expected for Core 24 from the geocentric axial dipole model (whereas the average characteristic remanence inclination was 53.8°). The same two-step procedure using the pelagic mud of Site 578 provided an estimate of the average magnetite particle anisotropy, $ARM_i/ARM = 0.550$ with 95% confidence interval +0.050/-0.090. This in turn is used to estimate $I_H = 54.0°$ with 95% confidence interval +4.3/-4.7 for Site 578. This contains the 53.4° field inclination expected from the geocentric axial dipole model (whereas the average characteristic remanence inclination was 48.8°). These results add further support to the applicability of this method of using Equation 1.1 for correcting for compaction-induced inclination shallowing.

According to the theory of Jackson et al. (1991), this method of correcting for inclination shallowing should be applicable whatever the domain state of the magnetite. The method requires soft sediment, preferably clay-rich to allow plastic deformation. However, with lithified sediment, it may be possible to disaggregate the sediment, remove the magnetite and mix it with clay to perform the compression experiments.

## 6.2 Correcting for Inclination Shallowing using Susceptibility Anisotropy and Uniaxial Compression Experiments

The above method of correcting for inclination shallowing was modified to use susceptibility anisotropy in place of remanence anisotropy. This is not expected to be

as reliable, but avoids the very time-consuming measurement of remanence anisotropy. We expect that the susceptibility anisotropy parameter ($K_{min}/K_{max}$) should (like $ARM_{min}/ARM_{max}$) be approximately linearly related to $\tan I/\tan I_H$ provided that the magnetite grains in the sediment are not single domain (Hodych et al., 1999). That is, we expect: $\tan I/\tan I_H \approx C(K_{min}/K_{max}) + 1 - C$ (where C is the slope of a regression line through experimental data on a plot of $\tan I/\tan I_H$ versus $K_{min}/K_{max}$) for our three sediment cores, all of which are dominated by pseudo-single-domain magnetite.

Six incremental four-step compression experiments were performed using a composite sample from Core 28 that was given an inclined ARM and was compressed in four stages from a 2 cm sphere to disk of 1.625 cm thickness, then 1.250 cm, then 0.875 cm and finally 0.500 cm thickness. The inclination of the remanence and the susceptibility anisotropy were measured at each stage and a linear correlation (Figure 4.6) was found between $\tan I/\tan I_H$ and $K_{min}/K_{max}$ as expected according to Hodych et al. (1999). The slope of the correlation line ($C = 2.19$ with 95% confidence interval $\pm 0.012$) was used in the equation $\tan I/\tan I_H \approx C(K_{min}/K_{max}) + 1 - C$ along with the original $I$ and $ARM_{min}/ARM_{max}$ values from the suite of natural specimens of Core 28 to estimate an average $I_H = 57.8°$ with 95% confidence interval +3.5/-3.4. This estimate includes the 60.6° field inclination predicted by the GAD model.

For the composite samples from Core 24 and Site 578, the susceptibility

anisotropy parameter $K_{min}/K_{max}$ was measured during two-step compression experiments. The slope of a trendline on a plot of $\tan I/\tan I_H$ versus $K_{min}/K_{max}$ is used to estimate $I_H$. For Core 24, this yields an estimate of $I_H$ = 59.0° with 95% confidence interval +4.7/-4.8. This estimate includes the 61.1° field inclination expected from the GAD model. For Site 578, this yields an estimate of $I_H$ = 53.1° for the suite of specimens (with 95% confidence interval +4.9/-5.0). This is contains the 53.4° field inclination expected from the GAD model.

This method is much less time-consuming than that using remanence anisotropy and seems to be almost as effective in correcting for inclination shallowing in our cores. However, it is not as reliable. For example, it cannot be used if a significant proportion of the magnetite is in single-domain grains.

## 6.3 Estimating Compaction-Induced Paleointensity Errors Using Magnetic Anisotropy and Uniaxial Compression Experiments

Burial compaction of a magnetite-bearing sediment can also reduce its remanence intensity. This can affect the sedimentary record of variation in paleointensity of the Earth's magnetic field but has received little study. We use empirical observations of the effect of uniaxial compression on remanence intensity and magnetic anisotropy in a composite sample to explore a new method of estimating the effect of burial compaction on remanence intensity in sediments.

We observed (Figure 5.1) a linear correlation between remanence intensity and remanence anisotropy parameter $ARM_{min}/ARM_{max}$ during two-step compression of a composite sample of Core 28 from a 2 cm diameter sphere to 1.0 cm and 0.5 cm thickness. Assuming the same relation held true in the natural sediment during burial compaction, it is possible to use the equation of the correlation line to estimate the remanence intensity prior to burial compaction using the original $ARM_{min}/ARM_{max}$ and remanence intensity data for each natural specimen from Core 28. Each result is then corrected for any variation in magnetite content from specimen to specimen by dividing these estimated remanence intensity values by the anhysteretic susceptibility, $K_{arm}$. This yielded a plot of relative paleointensity (corrected for compaction) versus depth in Core 28 (the dashed line in Figure 5.2).

A linear relation was also observed between decreasing remanence intensity and increasing susceptibility anisotropy parameter $K_{min}/K_{max}$ for the Core 28 composite sample. This and the $K_{min}/K_{max}$ and remanence intensity data for each natural specimen were used to estimate remanence intensity prior to compaction. Dividing by $K_{arm}$ gave the resultant plot of relative paleointensity (corrected for compaction) versus depth in Core 28 (the dotted line in Figure 5.2).

Two-step compression experiments were also done for the composite samples from Core 24 and Site 578. The trendlines on plots of remanence intensity versus $ARM_{min}/ARM_{max}$ and $K_{min}/K_{max}$ were used in the same way as the corresponding

correlation lines for the Core 28 composite sample to estimate paleointensity. The resultant plots of paleointensity (corrected for compaction) versus depth in the core are shown by the dashed line (using remanence anisotropy) and dotted line (using susceptibility anisotropy) in Figures 5.5 and 5.7.

The age of the sediments in these cores is not well enough known to test whether these corrections for compaction-induced reduction in paleointensity estimates are consistent with what is known about the past variation in the Earth's magnetic field strength. However, they do suggest that the compaction-induced reduction can be very significant and that compaction-induced magnetic anisotropy (particularly remanence anisotropy) may allow reliable corrections to be made.

## REFERENCES


Anson, G.L. and K.P. Kodama, 1987. Compaction-induced inclination shallowing of the post-depositional remanent magnetization in a synthetic sediment. *Geophys. J. R. Astron. Soc.*, 88, pp. 673-692.

Arason, P. and S. Levi, 1990. Models of inclination shallowing during sediment compaction. *J. Geophys. Res.*, 95, pp. 4481-4499.

Bijaksana, S., 1996. *Magnetic anisotropy and correction of paleomagnetic inclination shallowing in deep-sea sediments.* Ph.D. Thesis, Memorial University of Newfoundland, St. John's.

Bijaksana, S. and J.P. Hodych, 1997. Comparing remanence anisotropy and susceptibility anisotropy as predictors of paleomagnetic inclination shallowing in turbidites from the Scotian Rise. *Phys. Chem. Earth*, 22, pp. 189-193.

Butler, R.F. 1992. *Paleomagnetism: Magnetic Domains to Geological Terranes.* Blackwell Scientific Publications. Cambridge Massachusetts. 320p.

Deamer, G.A. and K.P. Kodama, 1990. Compaction-induced inclination shallowing in synthetic and natural clay-rich sediments. *J. Geophys. Res.*, 95, pp. 4511-4529.

Day, R., M. Fuller and V.A. Schmidt, 1977. Hysteresis properties of titanomagnetites: grain size and compositional dependence. *Phys. Earth Planet. Inter.*, 13, pp. 260-267.

Hodych, J.P. and S. Bijaksana, 1993. Can remanence anisotropy detect paleomagnetic inclination shallowing due to compaction? A case study using Cretaceous deep-sea limestones. *J. Geophys. Res.*, 98, pp. 22429-22441.

Hodych, J.P. and S. Bijaksana, 2002. Plastically deforming clay-rich sediment to help measure the average remanence anisotropy of its individual magnetic particles, and correct for paleomagnetic inclination shallowing. *Phys. Chem.Earth*, 27, pp. 1273-1279.

Hodych, J.P., S. Bijaksana and R. Patzold, 1999. Using magnetic anisotropy to correct for paleomagnetic inclination shallowing in some magnetite-bearing deep-sea turbidites and limestones. *Tectonophysics*, 307, pp. 191-205.

Jackson, M.J., S.K. Banerjee, J.A. Marvin, R. Lu and W. Gruber, 1991. Detrital remanence, inclination errors and anhysteretic remanence anisotropy: quantitative model and experimental results. *Geophys. J. Int.*, 104, pp. 95-193.

Johnson, E.A, T. Murphy and O.W. Torreson, 1948. Pre-history of the Earth's magnetic field. *Terr. Magn. Atmos. Elec.*, 53, pp. 349-372.

Kirschvink, J.L., 1980. The least squares line and plane and the analysis of paleomagnetic data. *Geophys. J. R. Astron. Soc.*, 62, pp. 699-718.

Kodama, K.P., 1997. A successful rock magnetic technique of correcting paleomagnetic inclination shallowing: case study of the Naciemento Formation, New Mexico. *J. Geophys. Res.*, 102B, pp. 5193-5205.

Kodama, K.P. and J.M. Davi, 1996. A compaction correction for the paleomagnetism of the Cretaceous Pigeon Point Formation of California. *Tectonics*, 14, pp. 1153-1164.

Kodama, K.P. and W.W. Sun, 1990. SEM and magnetic fabric study of a compacting sediment, *Geophys. Res. Lett.*, 17, pp. 795-798.

Mendenhall, W. and T. Sincich. 1986. *A Second Course in Business Statistics: Regression Analysis, Second Edition*. Dellen Publishing Company, California. 793p.

Merrill, R.T., M.W. McElhinny and P.L. McFadden, 1996. *The Magnetic Field of the Earth: Paleomagnetism, the Core, and the Deep Mantle*. Academic Press, Inc.. San Diego, California. 531p.

Stephenson, A., S. Sadikun and D.K. Potter, 1986. A theoretical and experimental comparison of the anisotropies of magnetic susceptibility and remanence in rocks and minerals. *Geophys. J. R. Astron. Soc.*, 84, pp. 185-200.

Tan, X. and K.P. Kodama, 1998. Compaction-corrected inclinations from southern California Cretaceous marine sedimentary rocks indicate no paleolatitudinal offset for the Peninsular Ranges terrane. *J. Geophys. Res.*,103B, pp. 27169-27192.

Tauxe, L., 1993. Sedimentary records of relative paleointensity of the geomagnetic field: Theory and practice. *Review of Geophysics*. 31, 3, pp. 319-354.

Appendix A

## PALEOMAGNETIC DATA

The following tables contain detailed paleomagnetic and rock magnetic data measured by Bijaksana (1996) and used in the present study. The first column identifies the specimen taken from the piston core. The second column gives the depth of the specimen in the piston core. The third column gives the inclination of the characteristic remanence, which is used as the observed remanence inclination, $I_o$ in this study. The fourth column gives the intensity of the natural remanent magnetization (NRM). The fifth column gives the anhysteretic susceptibility, $K_{arm}$, a dimensionless parameter defined as mean ARM divided by the strength of the biasing field. The sixth column gives the average of magnetic susceptibility $K_{mean} = (K_{max} + K_{int} + K_{min})/3$ in SI units. The seventh column gives the remanence anisotropy parameter $ARM_{min}/ARM_{max}$. The last column gives the magnetic susceptibility anisotropy parameter $K_{min}/K_{max}$.

**AGC Core HUD88010 no. 28** *(41°32.65'N, 62°15.04'W)*

| Sample | Depth (m) | Inclination of ChRM (°) | NRM Intensity (A/m) (e-2) | $K_{arm}$ (e-3) | $K_{mean}$ (e-7) | $ARM_{min}/ARM_{max}$ | $K_{min}/K_{max}$ |
|---|---|---|---|---|---|---|---|
| 28-0475 | 4.75 | 54.8 | 4.463 | 1.861 | 3.353 | 0.842 | 0.926 |
| 28-0515 | 5.15 | 56.7 | 5.146 | 2.771 | 3.824 | 0.829 | 0.899 |
| 28-0535 | 5.35 | 55.5 | 5.416 | 2.643 | 3.308 | 0.818 | 0.901 |
| 28-0565 | 5.65 | 51.4 | 4.128 | 1.862 | 3.921 | 0.812 | 0.892 |
| 28-0575 | 5.75 | 46.0 | 5.943 | 2.796 | 4.335 | 0.805 | 0.873 |
| 28-0605 | 6.05 | 53.5 | 6.222 | 2.734 | 5.055 | 0.859 | 0.907 |
| 28-0615 | 6.15 | 48.7 | 6.039 | 2.842 | 4.345 | 0.852 | 0.892 |
| 28-0674 | 6.74 | 40.0 | 5.981 | 2.792 | 4.581 | 0.856 | 0.877 |
| 28-0694 | 6.94 | 45.8 | 6.499 | 2.405 | 3.905 | 0.758 | 0.839 |
| 28-0714 | 7.14 | 42.7 | 7.000 | 2.454 | 3.951 | 0.816 | 0.853 |
| 28-0765 | 7.65 | 40.8 | 3.087 | 1.775 | 4.317 | 0.884 | 0.941 |
| 28-0775 | 7.75 | 52.0 | 5.032 | 2.207 | 3.844 | 0.885 | 0.937 |
| 28-0794 | 7.94 | 62.8 | 3.616 | 2.649 | 3.948 | 0.890 | 0.933 |
| 28-0816 | 8.16 | 56.5 | 3.792 | 2.435 | 3.573 | 0.868 | 0.930 |
| 28-0877 | 8.77 | 57.9 | 3.445 | 2.088 | 2.832 | 0.807 | 0.888 |
| 28-0896 | 8.96 | 55.4 | 2.869 | 1.457 | 2.126 | 0.863 | 0.926 |
| 28-0917 | 9.17 | 64.4 | 5.814 | 3.024 | 4.417 | 0.897 | 0.951 |
| 28-0976 | 9.76 | 51.3 | 6.449 | 3.956 | 4.736 | 0.886 | 0.910 |
| 28-0995 | 9.95 | 34.0 | 6.710 | 4.533 | 5.058 | 0.785 | 0.845 |
| 28-1075 | 10.75 | 57.2 | 6.496 | 3.859 | 4.34 | 0.866 | 0.899 |
| 28-1116 | 11.16 | 58.0 | 6.798 | 3.854 | 4.312 | 0.832 | 0.906 |
| 28-1125 | 11.25 | 55.2 | 5.584 | 3.851 | 4.609 | 0.845 | 0.939 |

**AGC Core HUD88010 no.24** *(42°10.25'N, 62°36.14')*

| Sample | Depth (m) | Inclination of ChRM (°) | NRM Intensity (A/m) (e-2) | $K_{arm}$ (e-3) | $K_{mean}$ (e-7) | $ARM_{min}/ARM_{max}$ | $K_{min}/K_{max}$ |
|---|---|---|---|---|---|---|---|
| 24-0403 | 4.03 | 62.5 | 3.807 | 2.242 | 3.362 | 0.829 | 0.883 |
| 24-0426 | 4.26 | 56.9 | 3.841 | 2.412 | 3.935 | 0.881 | 0.938 |
| 24-0446 | 4.46 | 58.9 | 3.376 | 2.305 | 3.426 | 0.892 | 0.928 |
| 24-0462 | 4.62 | 51.3 | 3.689 | 2.618 | 3.794 | 0.835 | 0.925 |
| 24-0486 | 4.86 | 54.7 | 5.123 | 2.616 | 3.777 | 0.893 | 0.936 |
| 24-0506 | 5.06 | 69.7 | 4.742 | 2.482 | 4.102 | 0.867 | 0.931 |
| 24-0526 | 5.26 | 68.8 | 4.629 | 3.074 | 4.386 | 0.905 | 0.950 |
| 24-0543 | 5.43 | 61.0 | 6.104 | 3.468 | 4.606 | 0.842 | 0.906 |
| 24-0562 | 5.62 | 68.9 | 6.256 | 3.846 | 4.807 | 0.888 | 0.933 |
| 24-0583 | 5.83 | 46.3 | 5.234 | 3.547 | 4.787 | 0.844 | 0.913 |
| 24-0604 | 6.04 | 49.8 | 6.144 | 4.110 | 4.661 | 0.868 | 0.926 |
| 24-0623 | 6.23 | 30.0 | 6.497 | 3.961 | 5.042 | 0.806 | 0.915 |
| 24-0642 | 6.42 | 46.2 | 4.953 | 4.342 | 4.834 | 0.884 | 0.931 |
| 24-0656 | 6.56 | 43.6 | 5.502 | 4.218 | 4.946 | 0.867 | 0.921 |
| 24-0677 | 6.77 | 52.2 | 4.432 | 2.417 | 3.034 | 0.893 | 0.930 |
| 24-0703 | 7.03 | 53.0 | 3.528 | 4.107 | 3.658 | 0.843 | 0.920 |
| 24-0742 | 7.42 | 59.0 | 4.189 | 3.263 | 3.554 | 0.865 | 0.912 |
| 24-0762 | 7.62 | 62.5 | 9.226 | 4.103 | 5.008 | 0.867 | 0.917 |
| 24-0783 | 7.83 | 51.1 | 9.330 | 4.798 | 4.843 | 0.770 | 0.866 |
| 24-0801 | 8.01 | 42.9 | 6.392 | 4.900 | 5.050 | 0.843 | 0.901 |
| 24-0816 | 8.16 | 40.1 | 3.837 | 4.295 | 4.330 | 0.860 | 0.919 |

**DSDP Site 578** *(33°55.56'N, 151°37.74'E)*

| Sample | Depth (m) | Inclination of ChRM (°) | NRM Intensity (A/m) (e-2) | $K_{arm}$ (e-3) | $K_{mean}$ (e-7) | $ARM_{min}/ARM_{max}$ | $K_{min}/K_{max}$ |
|---|---|---|---|---|---|---|---|
| 578-3-5-133 | 21.63 | 53.5 | 9.053 | 4.703 | 7.016 | 0.949 | 0.992 |
| 578-5-1-30 | 33.60 | 35.1 | 3.368 | 4.724 | 6.204 | 0.927 | 0.975 |
| 578-5-6-53 | 41.33 | 56.3 | 7.255 | 3.581 | 3.360 | 0.986 | 0.979 |
| 578-6-2-112 | 45.42 | 53.6 | 5.823 | 2.913 | 2.765 | 0.929 | 0.978 |
| 578-6-6-27 | 50.57 | 44.9 | 0.237 | 1.790 | 0.625 | 0.935 | 0.977 |
| 578-7-5-75 | 59.05 | 54.7 | 4.020 | 4.719 | 4.030 | 0.954 | 0.978 |
| 578-10-1-135 | 82.15 | 49.6 | 5.480 | 5.904 | 6.489 | 0.975 | 0.986 |
| 578-10-4-42 | 85.72 | 51.5 | 6.496 | 6.371 | 4.613 | 0.975 | 0.981 |
| 578-10-6-34 | 88.64 | 34.9 | 4.300 | 7.018 | 8.420 | 0.958 | 0.978 |
| 578-11-3-101 | 94.31 | 45.9 | 7.251 | 6.237 | 6.236 | 0.947 | 0.986 |
| 578-12-2-134 | 102.64 | 46.7 | 4.175 | 5.409 | 3.412 | 0.954 | 0.959 |
| 578-12-4-123 | 105.53 | 61.5 | 2.163 | 5.282 | 2.498 | 0.974 | 0.984 |
| 578-13-2-117 | 111.97 | 37.7 | 0.333 | 5.280 | 2.158 | 0.967 | 0.995 |
| 578-13-3-33 | 112.63 | 48.4 | 1.942 | 4.885 | 2.994 | 0.978 | 0.975 |
| 578-13-3-115 | 113.45 | 49.2 | 4.240 | 4.489 | 2.743 | 0.979 | 0.978 |
| 578-13-5-128 | 116.58 | 46.0 | 3.131 | 4.964 | 2.797 | 0.978 | 0.982 |

Appendix B

## EXPERIMENTAL DATA FOR SINGLE-STEP COMPRESSION EXPERIMENTS

The following tables contain detailed experimental data measured during the single-step compression experiments of the present study using core 28, core 24 and site 578. The first column identifies the experiment number. The second column gives the inclination, $I_H$, of the anhysteretic remanent magnetization (ARM) given to the randomized composite sample prior to compression. The third column gives the inclination, $I$, of the anhysteretic remanent magnetization after compression. The fourth column gives the tangent of $I$ divided by the tangent of $I_H$. The fourth column gives $J/J_o$, normalized intensity of the anhysteretic remanent magnetization (the intensity of magnetization after compression divided by the intensity of the magnetization prior to compression). The fifth column gives the remanence anisotropy parameter $ARM_{min}/ARM_{max}$ measured after compression. The last column gives the magnetic susceptibility anisotropy parameter $K_{min}/K_{max}$ after compression.

**Core 28**

**Half Compression (to 1 cm thickness) Trimming**

| Repeat No. | $I_H$ | $I$ | tan$I$/tan$I_H$ | J/J$_o$ | ARM$_{min}$/ARM$_{max}$ | K$_{min}$/K$_{max}$ |
|---|---|---|---|---|---|---|
| 1 | 57.6 | 50.6 | 0.773 | 0.717 | 0.880 | 0.904 |
| 2 | 60.2 | 57.0 | 0.882 | 0.747 | 0.892 | 0.920 |
| 3 | 61.5 | 49.2 | 0.629 | | 0.824 | 0.861 |
| 4 | 60.3 | 53.4 | 0.768 | | 0.839 | 0.876 |
| 5 | 61.3 | 53.7 | 0.745 | 0.610 | 0.841 | 0.866 |
| 6 | 58.7 | 47.4 | 0.661 | 0.658 | 0.845 | 0.872 |
| 7 | 57.9 | 47.9 | 0.694 | 0.647 | 0.843 | 0.882 |
| **Average** | 59.6 | 51.3 | 0.736 | 0.676 | 0.852 | 0.883 |

**Core 28**

**Full Compression (to 0.5 cm thickness) Trimming**

| Repeat No. | $I_H$ | $I$ | tan$I$/tan$I_H$ | J/J$_o$ | ARM$_{min}$/ARM$_{max}$ | K$_{min}$/K$_{max}$ |
|---|---|---|---|---|---|---|
| 1 | 60.3 | 49.1 | 0.658 | 0.133 | 0.699 | 0.761 |
| 2 | 60.2 | 42.1 | 0.517 | 0.143 | 0.743 | 0.785 |
| 3 | 58.7 | 45.9 | 0.627 | 0.115 | 0.690 | 0.763 |
| 4 | 60.6 | 38.4 | 0.447 | 0.085 | 0.741 | 0.758 |
| 5 | 60.0 | 42.0 | 0.520 | 0.119 | 0.692 | 0.764 |
| 6 | 60.8 | 43.7 | 0.534 | 0.119 | 0.693 | 0.761 |
| **Average** | 60.1 | 43.5 | 0.551 | 0.119 | 0.710 | 0.765 |

**Core 28**

**Full Compression (to 0.5 cm thickness) Stacking**

| Repeat No. | $I_H$ | $I$ | tan$I$/tan$I_H$ | J/J$_o$ | ARM$_{min}$/ARM$_{max}$ |
|---|---|---|---|---|---|
| 1 | 59.0 | 32.8 | 0.387 | 0.111 | 0.709 |
| 2 | 59.0 | 38.2 | 0.473 | 0.239 | 0.691 |
| 3 | 59.4 | 42.0 | 0.532 | 0.225 | 0.711 |
| 4 | 60.5 | 42.0 | 0.509 | 0.254 | 0.691 |
| 5 | 59.3 | 41.1 | 0.518 | 0.251 | 0.697 |
| 6 | 60.9 | 41.7 | 0.496 | 0.234 | 0.706 |
| **Average** | 59.7 | 39.6 | 0.486 | 0.219 | 0.701 |

**Core 24**

**Half Compression (to 1.0 cm thickness) Trimming**

| Repeat No. | $I_H$ | $I$ | tan$I$/tan$I_H$ | $J/J_o$ | $ARM_{min}/ARM_{max}$ | $K_{min}/K_{max}$ |
|---|---|---|---|---|---|---|
| 1 | 60.7 | 53.9 | 0.769 | 0.425 | 0.876 | 0.904 |
| 2 | 60.6 | 52.9 | 0.745 | 0.551 | 0.881 | 0.917 |
| 3 | 58.9 | 47.8 | 0.665 | 0.567 | 0.868 | 0.911 |
| 4 | 59.6 | 56.8 | 0.897 | 0.566 | 0.902 | 0.942 |
| 5 | 61.1 | 53.6 | 0.749 | 0.605 | 0.911 | 0.939 |
| 6 | 58.3 | 51.5 | 0.776 | 0.381 | 0.881 | 0.909 |
| **Average** | 59.9 | 52.8 | 0.767 | 0.516 | 0.887 | 0.920 |

**Core 24**

**Full Compression (to 0.5 cm thickness) Stacking**

| Repeat No. | $I_H$ | $I$ | tan$I$/tan$I_H$ | $J/J_o$ | $ARM_{min}/ARM_{max}$ | $K_{min}/K_{max}$ |
|---|---|---|---|---|---|---|
| 1 | 61.2 | 43.1 | 0.514 | 0.191 | 0.769 | 0.811 |
| 2 | 61.6 | 40.6 | 0.463 | 0.188 | 0.738 | 0.821 |
| 3 | 61.2 | 40.2 | 0.465 | 0.182 | 0.779 | 0.834 |
| 4 | 59.6 | 41.4 | 0.517 | 0.292 | 0.777 | 0.815 |
| 5 | 59.2 | 32.1 | 0.374 | 0.331 | 0.775 | 0.811 |
| 6 | 59.3 | 43.5 | 0.563 | 0.176 | 0.799 | 0.828 |
| **Average** | 60.4 | 40.2 | 0.483 | 0.227 | 0.773 | 0.820 |

**Site 578**

**Half Compression (to 1.0 cm thickness) Trimming**

| Repeat No. | $I_H$ | $I$ | tan$I$/tan$I_H$ | J/J$_o$ | ARM$_{min}$/ARM$_{max}$ | K$_{min}$/K$_{max}$ |
|---|---|---|---|---|---|---|
| 1 | 55.8 | 50.6 | 0.827 | 0.501 | 0.979 | 0.988 |
| 2 | 57.3 | 52.0 | 0.822 | 0.508 | 0.933 | 0.976 |
| 3 | 54.8 | 48.9 | 0.808 | 0.517 | 0.982 | 0.980 |
| 4 | 54.7 | 50.9 | 0.871 | 0.477 | 0.951 | 0.977 |
| 5 | 55.7 | 53.6 | 0.925 | 0.465 | 0.948 | 0.977 |
| 6 | 56.4 | 54.8 | 0.942 | 0.493 | 0.957 | 0.967 |
| **Average** | 55.8 | 51.8 | 0.866 | 0.494 | 0.958 | 0.978 |

**Site 578**

**Full Compression (to 0.5 cm thickness) Stacking**

| Repeat No. | $I_H$ | $I$ | tan$I$/tan$I_H$ | J/J$_o$ | ARM$_{min}$/ARM$_{max}$ | K$_{min}$/K$_{max}$ |
|---|---|---|---|---|---|---|
| 1 | 59.2 | 46.4 | 0.626 | 0.330 | 0.917 | 0.952 |
| 2 | 61.1 | 41.4 | 0.487 | 0.278 | 0.923 | 0.956 |
| 3 | 59.1 | 43.5 | 0.568 | 0.318 | 0.898 | |
| 4 | 62.5 | 49.5 | 0.610 | 0.234 | 0.910 | 0.956 |
| 5 | 60.3 | 42.7 | 0.526 | 0.300 | 0.902 | 0.956 |
| 6 | 61.1 | 45.6 | 0.564 | 0.283 | 0.898 | |
| **Average** | 60.6 | 44.9 | 0.563 | 0.291 | 0.908 | 0.955 |

Appendix C

## EXPERIMENTAL DATA FOR FOUR-STEP INCREMENTAL COMPRESSION EXPERIMENTS

The following table contains detailed experimental data measured during the four-step incremental compression experiments of the present study using core 28. The first column identifies the experiment number, each experiment consisting of five rows of data for each of five stages of the experiment (ie. the starting state and four subsequent compressions). The second column gives the thickness to which the sample was compressed during that step. (The first step, 2.0 cm, indicates the starting uncompressed thickness.) The third column gives the inclination of the anhysteretic remanent magnetization, *I*, after compression of the sample to the thickness for that step of the experiment. The fourth column gives the tangent of the inclination of the anhysteretic remanent magnetization of the sample after compression to the thickness indicated at that step divided by the tangent of the initial inclination. The fifth column gives the normalized intensity of the anhysteretic remanent magnetization which is normalized to its intensity prior to compression. The sixth column gives the magnetic susceptibility anisotropy parameter $K_{min}/K_{max}$ after compression and the last column gives the mean susceptibility $K_{mean} = (K_{max} + K_{int} + K_{min})/3$.

## Core 28

| | Disk Thickness (cm) | I (degrees) | tanI/tanIH | J/Jo | Kmin/Kmax |
|---|---|---|---|---|---|
| Experiment 1 | 2.000 | 60.2 | 1.000 | 1.000 | 1.000 |
| | 1.625 | 55.5 | 0.833 | 0.782 | 0.948 |
| | 1.250 | 47.5 | 0.625 | 0.636 | 0.882 |
| | 0.875 | 44.6 | 0.565 | 0.499 | 0.827 |
| | 0.500 | 43.6 | 0.545 | 0.415 | 0.782 |
| Experiment 2 | 2.000 | 60.7 | 1.000 | 1.550 | 1.000 |
| | 1.625 | 57.6 | 0.884 | 1.175 | 0.913 |
| | 1.250 | 51.2 | 0.698 | 0.952 | 0.866 |
| | 0.875 | 48.1 | 0.625 | 0.614 | 0.812 |
| | 0.500 | 42.9 | 0.521 | 0.439 | 0.774 |
| Experiment 3 | 2.000 | 60.8 | 1.000 | 1.503 | 1.000 |
| | 1.625 | 56.1 | 0.832 | 1.222 | 0.922 |
| | 1.250 | 51.9 | 0.713 | 0.994 | 0.875 |
| | 0.875 | 49.3 | 0.650 | 0.497 | 0.807 |
| | 0.500 | 45.0 | 0.559 | 0.424 | 0.775 |
| Experiment 4 | 2.000 | 60.8 | 1.000 | 1.003 | 1.000 |
| | 1.625 | 57.1 | 0.864 | 0.810 | 0.953 |
| | 1.250 | 53.4 | 0.753 | 0.663 | 0.889 |
| | 0.875 | 48.2 | 0.625 | 0.509 | 0.827 |
| | 0.500 | 45.3 | 0.565 | 0.418 | 0.774 |
| Experiment 5 | 2.000 | 59.6 | 1.000 | 1.513 | 1.000 |
| | 1.625 | 55.8 | 0.863 | 1.216 | 0.910 |
| | 1.250 | 49.5 | 0.687 | 0.980 | 0.851 |
| | 0.875 | 43.8 | 0.563 | 0.788 | 0.798 |
| | 0.500 | 35.5 | 0.418 | 0.419 | 0.758 |
| Experiment 6 | 2.000 | 61.8 | 1.000 | 1.520 | 1.000 |
| | 1.625 | 56.3 | 0.804 | 1.250 | 0.942 |
| | 1.250 | 52.2 | 0.691 | 1.010 | 0.885 |
| | 0.875 | 48.3 | 0.602 | 0.771 | 0.821 |
| | 0.500 | 40.5 | 0.458 | 0.647 | 0.789 |

Appendix D

# DERIVATION OF THE LINEAR RELATION BETWEEN INCLINATION SHALLOWING AND REMANENCE ANISOTROPY AS GIVEN IN EQUATION 4.2

Given the linear relation between $\tan I/\tan I_H$ vs $ARM_{min}/ARM_{max}$:

$$\text{slope } m = B$$

$$y = \frac{\tan I}{\tan I_H}$$

$$x = \frac{ARM_{min}}{ARM_{max}}$$

when isotropic: $y = 1$, $x = 1$

so $y = mx + b$ becomes $1 = m + b$, or $b = 1 - m$

therefore $y = mx + b$ becomes $y = mx + 1 - m$

Therefore:

$$\boxed{\frac{\tan I}{\tan I_H} = B\frac{ARM_{min}}{ARM_{max}} + 1\text{-}B}$$

Appendix E

## THE PEARSON PRODUCT MOMENT COEFFICIENT OF CORRELATION, *R*, AND A TABLE OF CRITICAL VALUES

One may test for a linear relationship between two variables using the Pearson product moment coefficient of correlation, *R*. The test statistic *R* must be greater than the critical value as given in the table below for a given sample size and confidence level. A correlation is assumed to exist with 95% confidence if:

$$R > \left( \frac{t_{\alpha/2}}{\sqrt{t_{\alpha/2}^2 + (n-2)}} \right)$$

where $t_{\alpha/2}$ = Student's t for $\alpha/2 = 0.025$ and $n$-2 degrees of freedom.

| Sample Size, *n* | *R*, 95% Confidence |
|---|---|
| 3 | 0.9969 |
| 4 | 0.950 |
| 5 | 0.878 |
| 6 | 0.811 |
| 7 | 0.754 |
| 8 | 0.707 |
| 9 | 0.666 |
| 10 | 0.632 |
| 11 | 0.602 |
| 12 | 0.576 |
| 13 | 0.553 |
| 14 | 0.532 |
| 15 | 0.514 |
| 16 | 0.497 |
| 17 | 0.482 |
| 18 | 0.468 |
| 19 | 0.456 |
| 20 | 0.444 |
| 21 | 0.433 |
| 22 | 0.423 |
| 27 | 0.381 |
| 32 | 0.349 |

The critical values of the Pearson product moment coefficient of correlation, *R*, for 95% confidence (abridged from Mendenhall and Sincich, 1986).

79 8170